Contract No:

This document was prepared in conjunction with work accomplished under Contract No. DE-AC09-08SR22470 with the U.S. Department of Energy (DOE) Office of Environmental Management (EM).

Disclaimer:

We put science to work.™

Savannah River National Laboratory™

OPERATED BY SAVANNAH RIVER NUCLEAR SOLUTIONS

A U.S. DEPARTMENT OF ENERGY NATIONAL LABORATORY • SAVANNAH RIVER SITE • AIKEN, SC

Preliminary Analysis of Species Partitioning in the DWPF Melter - Sludge Batch 7b

A. S. Choi

D. J. McCabe

June 2019

SRNL-STI-2018-00644, Revision 0

SRNL.DOE.GOV

DISCLAIMER

Printed in the United States of America

Prepared for
U.S. Department of Energy

SRNL-STI-2018-00644
Revision 0

Keywords: *DWPF Melter, Off-Gas Entrainment, Technetium, HTWOS Model*

Retention: *Permanent*

Preliminary Analysis of Species Partitioning in the DWPF Melter - Sludge Batch 7b

A. S. Choi

D. J. McCabe

June 2019

Prepared for the U.S. Department of Energy under contract number DE-AC09-08SR22470.

Savannah River National Laboratory™

OPERATED BY SAVANNAH RIVER NUCLEAR SOLUTIONS

REVIEWS AND APPROVALS

AUTHORS:

_____
Alexander S. Choi, Process Tech Programs/Wasteform Processing Tech/ES/SRNL Date

_____
Daniel J. McCabe, Wasteform Processing Tech/ES/SRNL Date

TECHNICAL REVIEW:

_____
Devon L. McClane, Immobilization Tech/Wasteform Processing Tech/SRNL Date

APPROVAL:

_____
G. A. Morgan, Manager Date
Process Tech Programs/Wasteform Processing Tech/ES/SRNL

_____
J. Manna, Director Date
Wasteform Processing Tech/Environmental Stewardship (ES)/SRNL

_____
C. C. Herman, Associate Laboratory Director Date
Environmental Stewardship (ES)/SRNL

ACKNOWLEDGEMENT

This work was performed as part of the Technetium Management Program Plan by the U.S. Department of Energy (DOE), Office of Environmental Management. We would like to thank Dr. Nicholas Machara of the Office of Technology Development for his continuing support of this work. We would also like to thank Brandon Hodges, Jim Coleman and Jeremiah Ledbetter of Savannah River Remediation (SRR) for their continuing support in terms of providing the DWPF operating data that formed the basis of this work and David McGuire of SRNL for interfacing with the SRR personnel for the necessary data collection. We would also like to recognize Fabienne Johnson of SRNL for compiling the analytical data for the Tank 40 sludge and glass pour stream samples in a spreadsheet for ready input into the model.

EXECUTIVE SUMMARY

The goal of the work described in this report is to provide additional off-gas carryover data from the Defense Waste Processing Facility (DWPF) melter to support the estimation of off-gas carryover rates from the Low Activity Waste (LAW) melter at the Hanford Site. Of particular interest is to determine the volatility of technetium-99 (Tc-99), which is a key isotope of concern for disposal and is a significant challenge to retain in glass in the Hanford waste treatment flowsheet. Since the DWPF melter is not equipped with routine off-gas monitoring and/or sampling capabilities, the off-gas carryover data had to be extracted using component mass balance of the measured feed and pour stream (PS) glass compositions under time-averaged melter operating conditions over the duration of one canister-filling cycle, typically 20-25 hours. The method was first tested using the Sludge Batch 6 (SB6) PS sample data taken while Canister #3472 was being filled on 12/20/2010, approximately three months after the (argon) glass bubblers were installed. The method was tested again using the SB7a PS sample data taken while Canister #3619 was being filled on 8/5/2011 with the glass bubblers in operation.

The analytical results of the PS sample provided the necessary glass composition for the mass balance. To estimate the "matching" feed composition, which is not necessarily the same as that of the Melter Feed Tank (MFT) content being fed at the time of PS sampling, a mixing model was developed by including the compositions of four preceding MFT batches as well as that being fed at that time of PS sampling. The model assumes perfect mixing in the melt pool but with an induction period to account for the process delays associated with the calcination and fusion of feed solids in the cold cap and thus reduced the number of melter turnovers for the last batch. Previous results of the SB6 and SB7a mass balance analysis showed that the proposed method of estimating off-gas carryover (or entrainment) rates from measured feed and PS sample compositions appeared feasible and thus additional case studies were recommended (SRNL-STI-2016-00540). This report documents the results of the SB7b mass balance analysis and compares them to the SB6 and SB7a results as well as the measured off-gas carryover data using the ⅓ scale Hanford LAW pilot melter at the Vitreous State Laboratory (VSL).

The DWPF has been in radioactive operation for over 22 years processing a wide range of high-level waste (HLW) feed compositions under diverse operating conditions, including bubbled vs. non-bubbled, feeding vs. idling, and varying feed rates and solids loading. It is thus desirable to find out how the varying feed compositions and operating parameters impacted the off-gas carryover rates of individual species as well as the overall rate. However, as it is not feasible to measure the off-gas carryover rates directly, the proposed method provides an indirect way of extracting the data; it is a series of mass balance calculations used to estimate off-gas carryover rates from available feed and PS sample characterization and melter operating data. This calculation method was tested further in this study using the SB7b PS glass data taken while Canister #4023 was being filled over a 26-hr period between 3/18/2013 and 3/19/2013 also with the glass bubblers in operation. In doing so, several changes were made to the mass balance method used in the SB6 and SB7a analysis to more accurately interpret and apply available DWPF operating data.

First, the mixing model was expanded to include the effect of heels on the MFT composition using the MFT level data. Second, the calcine ratio and the frit-fractions of measured Si, Li, and Na concentrations in each MFT batch were calculated from their respective Slurry Mix Evaporator (SME) data using the mixing model, including the heels. Third, the estimated total solids (TS) and density data provided by the DWPF personnel at the beginning and end of each MFT batch were checked against the measured data for one of the five MFT batches considered in the mass balance and, if necessary, adjustments were made to the total solids of the remaining batches using the density-vs-TS correlation derived from the compiled SME/MFT data. Fourth, the calcine solids and slurry volume balances were performed as accurately as data would allow for each MFT batch in order to calculate the adjustment factor for the measured slurry feed rate so that the adjusted feed rate would match that calculated from the MFT level changes. Fifth, the waste loading

(WL) of the PS glass was calculated from the measured composition and found to be significantly different from that of the projected glass composition at the time of PS sampling. This necessitated the adjustment of the PS glass composition until the resulting WL matched the projected value based on the reported WLs of the SME batches. In doing so, the Measurement Acceptability Region (MAR) assessment was done on the adjusted PS glass composition to ensure that it still met all DWPF glass constraints.

Another way to reconcile the large WL difference between the projected and measured glass compositions would be to override the reported WLs of all SME batches from the Product Composition Control System (PCCS) analysis and vary them simultaneously until the WL of the projected glass composition equaled that of the PS sample, 36.8%. Since the PCCS WLs were set based on the fixed sludge oxides/Fe ratio of 5.75 for SB7b, they could be adjusted by changing either the sludge oxides loading in Tank 40 or the Fe concentration in the SME. Since Fe was the third most abundant species after Si and Na, it would have been difficult to justify adjusting it alone and, even then, it must be adjusted for all five SME batches as its measured concentrations remained relatively steady. It means that adjusting the Fe concentrations would be more arbitrary and thus more difficult than adjusting the PS sample composition and, not to mention, it requires that charge reconciliation be redone. The other option of adjusting the sludge oxides loading would be simpler; however, it would mean overriding the results of the Tank 40 Waste Acceptance Preliminary Specifications (WAPS) sample analysis. Regardless, since the off-gas carryover rate of each element was calculated as the difference between its feed and glass pour rates, adjusting the PCCS WLs (and thus the feed composition) vs. adjusting the PS sample composition would likely produce similar carryover results at the given overall feed and glass pour rates.

The results of the SB7b mass balance analysis showed that:

1. The proposed method of estimating off-gas carryover (or entrainment) rates from measured feed and pour stream glass compositions appears feasible and thus additional case studies are warranted. However, success of this approach requires that the analytical data for the feed and pour stream glass be both accurate and consistent and all relevant melter operating data be interpreted, analyzed, and applied correctly.

2. The overall SB7b entrainment rate from the bubbled DWPF melter was calculated to be 1.5% of the calcine solids fed based on the mass balance between the total calcine solids fed and the total glass poured over five MFT batches. This rate is 50% higher than the design basis entrainment rate for the non-bubbled melter but is in line with recent results of SB6 and SB7a.

3. The sum of the elemental carryover rates of five major nonvolatile sludge components, i.e., Al, Fe, Mn, Ni, and U, was 5.2%, while that of the frit components, including Si, B, Li but not Na, was 2.1%. The calculated carryover rate of 5.2% for the sludge group is skewed high because that of Fe was high at 6.8%; Fe accounted for 43% of the major sludge components at concentration >1%.

4. The sludge/frit mass ratio in the off-gas carryover was 2X that in the MFT661, which indicates that the relative carryover tendency of the sludge as a group was 2X that of the frit. By comparison, the sludge/frit mass ratio in the quencher deposit sample taken in 2007 was 7X that in the SME388 that was fed in December 2006 as part of SB3, which is consistent with the SB7b results; the sludge was more prone to carryover than the frit. Since the main difference in the DWPF melter operation between 2007 and 2013 was the use of glass bubblers during SB7b but not during SB3, the much lower sludge/frit mass ratio in the SB7b carryover suggests that the frit particles are comparatively more prone to carryover than the sludge counterparts when the glass bubblers are in use.

5. When the measured glass REDOX (i.e., $Fe^{2+}/\Sigma Fe$) was decreased from 0.13 (SB7a) to 0.07 (SB7b), the calculated carryover rate of Tc-99 increased from <60.2% to 84.3%, as would be expected under more oxidizing conditions.

6. The calculated carryover rate of Cs-137 was 14.2%, which means that the carryover rate of Cs-137 remained relatively steady between 13.6% (SB7a) and 16.4% (SB6) regardless of the bubbling flux, REDOX and WL tested.

7. The calculated carryover rate of sulfur was unexpectedly low at 8%, compared to >49% for SB6. It is suspected that the low SB7b carryover rate of S also may have been affected by the seemingly-biased PS glass composition, as discussed later in the report.

8. The impact of bubbling flux on the carryover rate was not conclusive. When the bubbling flux was decreased from 0.18 scfm/ft^2 (SB6) to 0.15 scfm/ft^2 (SB7b), the calculated carryover rates of Al, B, Na, Cs-137, Th-232 and $\Sigma U_{isotope}$ all decreased, as expected. However, Fe and Si showed the opposite trend. Tc was below detection limit in the SB6 glass so could not be compared.

9. The results of the FactSage code run with SME Batch 660 (SME660) composition showed that:

    9-1. 100% of Cs and Tc would volatilize as $CsBO_2$/CsCl and Tc_2O_7, respectively, under the thermodynamic equilibrium conditions at 1,100 °C. These predicted rates represent the thermodynamic maximum in the absence of any mass transfer resistances such as the presence of the cold cap and bulk diffusion through the glass melt.

    9-2. The predicted volatilities of U and Th were essentially zero, which means that the low but non-zero carryover rates of U and Th-232 calculated based on the SB7b data were likely due to physical entrainment rather than their relative volatilities.

    9-3. 7.3% of boron fed was predicted to volatilize as alkali borates vs. the calculated volatility of 1.3% based on SB7b data.

    9-4. The predicted REDOX of the SME660 glass was 0.059 vs. the PCCS-reported value of 0.056, i.e., they were essentially identical.

10. When compared against the measured off-gas carryover data during the DM1200 melter runs at the Vitreous State Laboratory (VSL), the calculated DWPF melter carryover rates of the major feed components were higher than their DM1200 counterparts by up to 7X (for Fe). Two main exceptions were B and S. The higher carryover rate of B from DM1200 is likely because boron was added as boric acid instead of more refractory B_2O_3, as in the DWPF Frit 418.

The uncertainty analysis of the results highlighted above was not performed in this study for two reasons. First, although the off-gas carryover rates of individual feed components were calculated as the difference between their respective feed and pour rates, which sounds simple, it requires both analytical and plant operating data taken under steady state conditions and their uncertainty bounds, especially those of the latter, are difficult to determine. Second, a true steady state operation is seldom achieved, if possible at all, in an actual production melter environment. For example, glass is not poured into a canister at a uniform rate for the duration of one-canister filling cycle and, to overcome this, the average pour rate is calculated based on the total glass poured and the time it took to fill each canister. However, if there was a net change in melt level before and after the pouring operation, the calculated pour rate needed to be adjusted accordingly to preserve the steady state assumption, i.e., a constant melt level. As stated above, the interpretation and application of the plant operating data in the mass balance analysis have been made more precise and thus

more relevant in this study in consultation with the DWPF personnel and additional work is clearly needed to eventually determine the uncertainty bounds of some of the key operating data, including the measured slurry density and total solids. Until then, the results presented in this report should be taken as "preliminary."

The path forward is to continue testing of the mass balance methodology against additional sludge batches, provided relevant analytical and operating data is available. The resulting database of calculated off-gas carryover rates will then be screened in terms of bubbling flux, percent idling time, REDOX, melt viscosity, vapor space height, etc. Once key design and operating variables are gleaned from DWPF data, a regression analysis coupled with the high-temperature thermodynamic modeling of calcination and fusion reactions will be performed on the entire database, both the calculated (from the DWPF melter data) and measured (during pilot-scale melter runs). The ultimate goal of this task is to develop correlations for predicting off-gas carryover rates from both the LAW and HLW melters of the Waste Treatment Plant (WTP) as a function of feed chemistry and key melter operating parameters and incorporate them into the TOPsim model as well as the dynamic flowsheet model based on the Gensym's G2® programming language.

TABLE OF CONTENTS

LIST OF TABLES xii
LIST OF FIGURES xii
LIST OF ACRONYMS xiii
1.0 Introduction 1
2.0 Description of Task 1
3.0 DWPF Flowsheet 3
4.0 Mixing Model of Melt Pool 4
5.0 Mass Balance Analysis 5
5.1 Mixing Models 5
5.1.1 MFT Composition with Heels 6
5.1.2 Melt Pool 6
5.2 Case Study: SB7b 7
5.2.1 Mass Balance Equations of SB7b 9
5.2.2 Feed Chemistry of SB7b 10
5.2.2.1 Charge Reconciliation of SME Product Data 10
5.2.2.2 Calculation of MFT Batch Composition 15
5.2.3 Mass Balance Calculations of SB7b 18
5.2.3.1 Bases and Assumptions 18
5.2.3.2 Calculation Steps 19
5.2.4 Results of SB7b Mass Balance 19
5.2.4.1 Calculated Melt vs. PS Sample Compositions 19
5.2.4.2 Off-Gas Carryover Rates and Adjustment of PS Sample Composition 22
5.2.4.3 Comparison of Overall Off-Gas Carryover Rates 24
6.0 Thermodynamic-Equilibrium Prediction of Off-Gas Carryover Rates 25
7.0 Discussion 27
7.1 Impact of Bubbling on Off-Gas Carryover 27
7.2 Impact of REDOX on Tc Volatility 29
7.3 Impact of Temperature on Off-Gas Carryover 29
7.4 Additional Factors Affecting Off-Gas Carryover 30
7.5 Additional Thoughts on Elemental Carryover Rates 30
7.6 Comparison with DM1200 Data 33

8.0 Conclusions 35
9.0 Future Work 36
10.0 Quality Assurance 36
11.0 References 37

LIST OF TABLES

Table 1. Operating History and MFT Batch Bulk Properties for SB7b Mass Balance [10-11]. 8

Table 2. Analytical Data Used in Charge Reconciliation of SME657-SME661. 11

Table 3. Results of Charge Reconciliation of SME Product Analytical Data. 12

Table 4. Charge-Reconciled Elemental Compositions of SME657-SME661 vs. Tank 40. 13

Table 5. Changes in Relative Concentrations with Respect to Fe from Tank 40 to SME. 14

Table 6. Calcined Solids and Calcination Ratios of MFT657-MFT661. 16

Table 7. Calculated Elemental Compositions of MFT657-MFT661 Including Heels. 17

Table 8. Operating Parameters and MFT580 Properties for SB7a Mass Balance Calculations. 18

Table 9. Calculated Elemental Compositions of MELT657-MELT661 vs. PS Sample. 20

Table 10. Predicted vs. Measured SB7b Glass compositions and Off-Gas Carryover Rates. 21

Table 11. Predicted vs. Measured SB7b Glass Isotopic Compositions and Off-Gas Carryover Rates. 23

Table 12. Comparison of Overall Off-Gas Carryover Rates. 24

Table 13. Pre-Decomposed SME660 Input to FactSage Run. 25

Table 14. Equilibrium Partitioning of SME660 Using FactSage v7.0 at 1,100 °C and DWPF Design Basis Glass Rate of 228 lb/hr 26

Table 15. Comparison of DWPF vs. DM1200 Melter Off-Gas Entrainment Ratios. 28

Table 16. Off-Gas Carryover vs. DWPF Glass WL 30

Table 17. Analytical Results of DWPF Quencher Deposit Sample (Data Taken from Ref. 6). 31

LIST OF FIGURES

Figure 1. Simplified DWPF Process Flow Diagram. 4

Figure 2. Measured Density vs. Total Solids of MFT/SME Samples of SB6, SB7a and SB7b. 9

LIST OF ACRONYMS

AR	Aqua Regia
ARP	Actinide Removal Process
CSSX	Caustic-Side Solvent Extraction
CT	Computed Tomography
DCS	Distributed Control System
DF	Decontamination Factor
DOE	Department of Energy
DWPF	Defense Waste Processing Facility
GPCP	Glass Product Control Program
GPM	Gallons per Minute
HLW	High-Level Waste
HTWOS	Hanford Tank Waste Operations Simulator
LSFM	Large-Slurry Fed Melter
LAW	Low-Activity Waste
MAR	Measurement Acceptability Region
MCU	Modular CSSX Unit
MFT	Melter Feed Tank
ORP	Office of River Protection
PCCS	Product Composition Control System
PF	Peroxide Fusion
PS	Pour Stream
REDOX	REDuction-OXidation
SB	Sludge Batch
SBS	Submerged Bed Scrubber
SME	Slurry Mix Evaporator
SRAT	Sludge Receipt and Adjustment Tank
SRNL	Savannah River National Laboratory
SRS	Savannah River Site
TIC	Total Inorganic Carbon
TOC	Total Organic Carbon
TSR	Technical Safety Requirement
VSL	Vitreous State Laboratory
WL	Waste loading
WTP	Waste Treatment Plant

1.0 Introduction

As part of the overall effort to support the technetium (Tc) management program at the Hanford Site,[1] this task seeks to develop an improved capability for predicting species partitioning in the Low Activity Waste (LAW) melter between the glass and off-gas carryover. Specifically, the aim is to develop correlations (or algorithms) for the off-gas carryover rates of several key species, including Tc-99 and Cs-137, in terms of feed chemistry and melter operating variables. The basis for doing so is the radioactive production melter data from the Defense Waste Processing Facility (DWPF) at the Savannah River Site (SRS), which began operation in 1996 and has since produced 4,179 glass canisters as of 1/16/2019, each containing about 3,800 lb of high-level waste (HLW) glass. The DWPF feed is prepared in large batches, each lasting typically for ~2 years, by blending varying volumes of waste from multiple storage tanks and the facility is currently processing the sludge batch 9 (SB9), which is the eleventh sludge batch including the sub-batches of SB1 and SB7. Just as the chemistry of the SBs processed thus far has been diverse, so have the conditions under which the DWPF melter has been operating - with or without the use of glass bubblers, varying feed rates, including zero cold cap coverage during idling, etc. Thus, the scope of the data collected for the last 22 years of melter operation is quite large.

As is the case with most production facilities, however, the DWPF melter is not equipped with routine off-gas monitoring and/or sampling capabilities, which means that off-gas carryover data can only be obtained indirectly, if possible at all. Thus, it was proposed that off-gas carryover rates be calculated based on the mass balance between the calcined feed and glass pour rates provided that their respective compositions are known. Central to this approach is that during each SB campaign the DWPF is required to take at least one glass sample to meet the objectives of the Glass Product Control Program (GPCP),[2] which is in turn governed by the DWPF Waste Form Compliance Plan.[3] The required glass sample is taken off the pour stream (PS) into a canister, which typically takes 20 to 25 hours to fill, and it is the analytical results of the PS sample that formed the necessary glass composition for the mass balance analysis under time-averaged melter operating conditions over the duration of one canister-filling cycle. To estimate the "matching" feed composition, which is not necessarily the same as that of the Melter Feed Tank (MFT) content being fed at the time of PS sampling, a mixing model was developed by including the compositions of four preceding MFT batches as well. The model assumes perfect mixing in the melt pool but with an induction period to account for the process delays involved in the calcination and fusion reactions in the cold cap and thus reduce the number of melter turnovers for the last batch.

The proposed method was first tested using the sludge batch 6 (SB6) PS sample data taken while Canister #3472 was being filled over a 20-hr period on 12/20/2010, approximately three months after the (argon) glass bubblers were installed.[4] The method was tested again using the SB7a PS sample data taken while Canister #3619 was being filled over a 21-hr period on 8/5/2011 also with the glass bubblers in operation.[5] The results of the SB6 and SB7a mass balance analysis showed that the proposed method of estimating off-gas carryover rates by utilizing measured feed and PS glass compositions under the time-averaged melter operating conditions appeared feasible and thus additional case studies were recommended (SRNL-STI-2016-00540). This report documents the estimated off-gas carryover rates of both major and minor species from the SB7b mass balance analysis and compares them to those of SB6 and SB7a as well as the measured melter emissions data from the ⅓ scale Hanford LAW pilot melter at the Vitreous State Laboratory (VSL).

2.0 Description of Task

The melter feed and glassy materials can enter the off-gas system in two ways. First, they can become airborne and entrained by a sudden surge of steam and calcine gases ejecting out of the cold cap. This physical mode of carryover is influenced by not only the melter design and operating variables such as glass bubbling rate but the feed chemistry and rheology as well. The other mode of carryover is chemical in

nature; some species such as CsCl becomes volatile at the nominal glass temperature of 1,150 °C and exit the melter as vapor only to condense into an aerosol when it cools downstream of the melter. Under normal feeding/pouring melter operation with a cold blanket of feed materials, called the cold cap, covering the melt surface, particulate carryover is dominated by physical entrainment, as shown by the analytical results of off-gas deposits consisting mainly of the non-volatile species by weight.[6] Under idling mode, however, particulate carryover decreases dramatically since off-gas carryover occurs by the volatility of each species. Thus, the off-gas carryover data from actual melter runs, either measured or extracted, would include both physical and volatility-driven entrainments.

The main goal of this task is to develop predictive tools for estimating off-gas carryover rates of key species of interest and integrate them into the LAW melter module of the Hanford tank waste operation simulator model, called TOPSim (previously called "HTWOS"). The tools will also be applicable to the HLW melter. A staged approach to achieving this goal is outlined in the task plan;[7] (1) understanding of the TOPsim model construct, (2) data mining on off-gas carryover (or entrainment) rates preferentially from large-scale melters, (3) thermodynamic modeling of the vitrification process to estimate the bounding off-gas carryover rates due to volatility particularly for the semi-volatile species, (4) empirical modeling of the overall as well as elemental off-gas carryover rates, (5) aqueous electrolyte modeling of the off-gas condensate chemistry, and (6) integration of the species partitioning algorithms into the TOPsim model. If necessary, the scope of Stage 6 will be expanded to include the integration into the G2® flowsheet model, which is similar to the TOPsim model in scope but built on the Gensym's G2® programming language.

Stage 1 and part of Stage 2 of the task plan listed above were completed in 2014. Specifically, the off-gas carryover data collected during Stage 2 came from two sources; (1) DM1200 melter runs at the VSL using both the HLW and LAW simulants for the Waste Treatment Plant (WTP) blended with glass-forming chemicals,[8] and (2) the Large Slurry-Fed Melter (LSFM) runs at the Savannah River National Laboratory (SRNL) using various DWPF sludge feed simulants blended with glass-forming frits.[9] (Note that only one representative reference is given for each melter instead of citing all reports from which off-gas carryover data was obtained.) Both DM1200 and LSFM were targeted since they are relatively large in scale, having the melt surface area equaling 42% to 45% of the DWPF melter, respectively. The off-gas sampling and analytical methods used in the two melter runs were also similar; off-gas was sampled isokinetically downstream of the film cooler and the particulate collected was characterized and quantified in terms of elemental mass balance. Off-gas carryover rates were measured under different conditions by varying the bubbling rate and/or the number of bubblers, feed chemistry, etc., and the data thus collected will form part of the basis for the empirical modeling in Stage 4.

The feasibility of expanding the range of carryover data collected in Stage 2 was assessed in earlier studies by including the DWPF melter data taken in a radioactive production environment during the processing of SB6 and SB7a.[4,5] The scope of available DWPF data is large but, as is the case with most manufacturing plants, data collection is geared toward production support through process control and troubleshooting. For example, the DWPF melter is equipped with comprehensive pressure, temperature, and flow control loops but not with routine off-gas sampling or monitoring capabilities, which means that off-gas carryover rates cannot be measured directly. Samples of off-gas system deposits and condensate had been collected and analyzed over the years but failed to yield necessary quantitative information for the estimation of species partitioning between the glass and off-gas carryover because data was not collected under any controlled conditions. The only remaining option was indirect estimation based on the component mass balance using measured feed and PS glass compositions; however, out of the typical duration of ~2 years for each SB, the latter limited the mass balance window to the specific time when the PS sample was taken. Thus, it was proposed that steady state mass balance be set up by simulating the time-averaged melter operating conditions at the time of PS sampling over the duration of one-canister filling cycle and the off-gas carryover rates be calculated as the differences between the component mass flows in the calcined feed and those in the PS as a representation of the entire SB.[7]

The proposed method was tested earlier using the feed and PS composition data for SB6 and SB7a,[4,5] and testing continued in this study using the SB7b PS sample data taken while Canister #4023 was being filled over a 26-hr period between 3/18/2013 and 3/19/2013 with the glass bubblers in operation. In doing so, several changes were made to the mass balance method used earlier to help interpret and apply available DWPF data more accurately particularly on the melter feed preparation and operation:

1. The mixing model was revised to include the effect of heels on the MFT batch composition using the MFT level data, as indicated by the level indicator LI3182 in the DWPF Distributed Control System (DCS).

2. The calcine ratio and frit-fractions of Na, Si, and Li in each MFT batch were calculated from their respective Slurry Mix Evaporator (SME) data using the revised mixing model.

3. The total solids and density data provided by the DWPF personnel at the beginning and end of each MFT batch were checked against the measured data for every 5th MFT batch and, if necessary, adjustments were made to the total solids of the remaining MFT batches using the density-vs-TS correlation derived from the compiled SME/MFT data.

4. The calcine solids and MFT slurry volume balances were done as accurately as data would allow to calculate the adjustment factor for the measured slurry feed rate, as indicated by the DCS flow controller output FIC3309 so that the adjusted FIC3309 would match that calculated based on the LI3182 data.

5. The waste loading (WL) of the PS glass was calculated from the measured PS composition and found to be significantly different from that of the projected MELT composition at the time of PS sampling. This necessitated the adjustment of the measured PS composition until the PS glass WL matched the projected value based on the reported WLs of the SME batches.

These changes are described in more detail later in this report and their varying degrees of impact on the calculated SB7b off-gas carryover rates are discussed in light of the data from external sources.

3.0 DWPF Flowsheet

Figure 1 shows a simplified flow diagram of the processing units, including the melter, which provides the bulk of the necessary process/operating data for this work. Tank 40 is a staging tank with over one million-gallon capacity where each washed sludge batch is stored before being fed to the DWPF. The composition of Tank 40 content is fully characterized, including a complete radioisotope analysis, as part of the sludge qualification process. The measured Tank 40 composition was used in this study as the reference point for estimating the concentrations of those species not measured in the SME product.

The Sludge Receipt and Adjustment Tank (SRAT) is where the sludge feed is received, neutralized with nitric acid and blended with input streams from the Modular CSSX Unit (MCU) and Actinide Removal Process (ARP). The pH of the SRAT content is further reduced by adding formic acid, which also acts as a reducing agent for HgO and MnO_2, and the content is boiled under total reflux for an extended period to steam strip Hg. The nitrite is also destroyed during the boil-up. The resulting SRAT product is analyzed for the elemental (including total U and Th), anions, total organic carbon (TOC), total inorganic carbon (TIC), and Cs-137 but no other radioisotopes. The analytical results of the SRAT product were used to cross-check the charge-reconciliation results of the SME product analytical data.

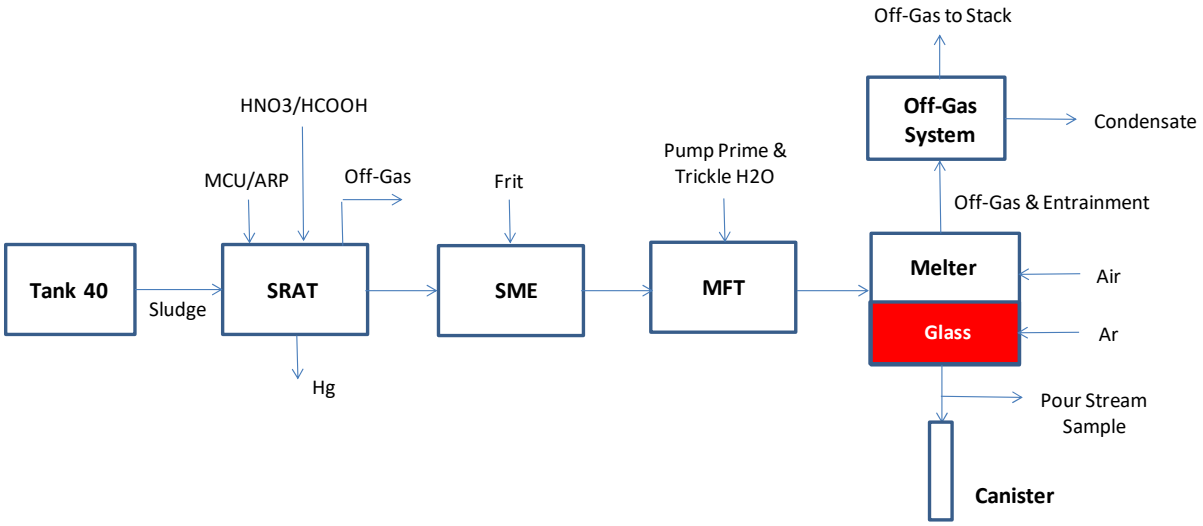

Figure 1. Simplified DWPF Process Flow Diagram.

The SRAT product is transferred to the SME in a ~4,500-gallon batch, blended with the glass-forming frit per the Product Composition Control System (PCCS) analysis and the content is boiled down to a target total solids.[31] The remaining SME content is sampled and analyzed for the elemental (including total U and Th), anions, TOC, and Cs-137 but no other radioisotopes. Once the Technical Safety Requirement (TSR) limits are met, the SME product is transferred to the MFT. While being fed to the melter, the MFT content is continually diluted every time the transfer pump is started up and by a constant trickle flow of water. The MFT content is sampled at every 5th batch and analyzed for pH, density and total solids only. Since no chemical reactions are expected to occur in the MFT, the compositions of the SME product and MFT content in principle should be the same on a dry basis, ignoring the effect of tank heel. As a result, the analytical results of each SME product were used in this study to develop the corresponding MFT batch composition, including the heels, which was adjusted further to account for the dilution by water additions prior to being fed to the melter.

4.0 Mixing Model of Melt Pool

The proposed method of estimating off-gas carryover rates as the difference between the calcined feed and glass pour rates of individual species (or the sum of all species for the overall entrainment rate) is based on the following assumptions:

1. The feeding and pouring operation is at steady state over one canister-filling cycle.

2. The glass (melt) level remains constant.

3. The mixing in the glass (melt) pool is perfect.

The duration of each canister-filling cycle is typically 20-25 hours. While the indicated feed rate (FIC3309) is likely to remain relatively constant during that time, the instantaneous glass pour rate fluctuates more especially near the end of a filling cycle. Assumption #1 enables use of the time-averaged feed/pour rates in the mass balance calculations. A constant glass level (Assumption #2) requires that the volumetric flow

rate of calcined solids entering the glass pool (from the cold cap) equal that of the glass being poured, which in essence implies zero off-gas carryover. However, as long as the overall carryover rate is not large (e.g., < ~5% fed), the measured glass level should remain relatively constant. Since the DWPF melter has a relatively large melt surface area of 28.3 ft^2, even a small change in glass level before and after the pour could translate into a significant mass of glass over- or under-accounted for in the estimation of steady state pour rate, and this assumption helps the estimated pour rate be in line with the measured calcine feed rate. For example, if there was a net decrease of 1 inch in glass level after the pour, the measured pour rate must be adjusted down by ~17 lb/hr, i.e., (350 lb glass/inch)(1 inch/21 hr), which is equivalent to ~9% of the nominal pour rate. Likewise, if there was a net increase in glass level, the measured pour rate must be adjusted up by the amount of glass above the initial glass level. The net level changes before and after the pour are typically small - on the order of 1-2% of the nominal glass of level of 32.7 inches.

Ideal mixing (Assumption #3) simplifies the calculation of the varying melt composition upon feeding successive MFT batches. One drawback is that the calcined/fused solids exiting the cold cap is assumed to blend into the melt pool instantly, which is not feasible considering the high viscosity of glass melt, which is three orders of magnitude or higher than that of water. To overcome this difficulty, a full glass residence time in the melt pool was subtracted in the calculation of melter turnover by the last batch,[4] which may have been excessive under the forced-convection mixing induced by the glass bubblers. The mixing delay was further examined during the SB7a study and judged to be too excessive; thus, it was dropped from the analysis.[5]

5.0 Mass Balance Analysis

In actual melter operation, the composition of glass being poured could be quite different from that of the calcined feed being fed at the same time for two main reasons. First, the feed composition can change appreciably from one MFT batch to the next even though the sludge feed originates from the same Tank 40 batch due to the potential inhomogeneity in Tank 40 content, and the timing and varying volumes of the MCU/ARP additions, etc. Second, even under the perfect-mixing scenario, it would take 4 to 5 melter turnovers to flush out over 99% of a given batch of feed. One melter turnover is defined here as when the cumulative volume of calcined solids fed equals one melt pool volume. At the nominal melt level of 32.7", the DWPF melter contains over 12,000 lb of glass, which is enough to fill three canisters, and the nominal glass residence time is on the order of 70 hours. Thus, in order to calculate the off-gas entrainment rates of individual elements as the difference between the feed and pour rates of a particular element, it is essential to know the composition of the "composite" feed spanning several MFT batches that is representative of the melt pool composition at the time of PS sampling but without entrainment. For that, a mixing model is required that accounts for the effects of melt pool volume (or holdup) and residence time as well as the incoming batch volume and composition on the glass composition.

5.1 Mixing Models

In addition to the mixing model of the melt pool, the effect of heel on the final MFT composition that is fed to the melter was accounted for by tracking both the MFT heel volume at the end of each batch and the maximum slurry volume at the completion of a new SME batch transfer.

5.1.1 MFT Composition with Heels

The concentration of species *i* in the MFT Batch 658 (MFT658) to MFT661 are calculated as follows:

$$x_i(658) = \frac{\left[x_i(657) * m_{heel}(657) + x_{SME,i}(658) * m_{SME}(658)\right]}{\left[m_{heel}(657) + m_{SME}(658)\right]} \quad (1)$$

$$x_i(659) = \frac{\left[x_i(658) * m_{heel}(658) + x_{SME,i}(659) * m_{SME}(659)\right]}{\left[m_{heel}(658) + m_{SME}(659)\right]} \quad (2)$$

$$x_i(660) = \frac{\left[x_i(659) * m_{heel}(659) + x_{SME,i}(660) * m_{SME}(660)\right]}{\left[m_{heel}(659) + m_{SME}(660)\right]} \quad (3)$$

$$x_i(661) = \frac{\left[x_i(660) * m_{heel}(660) + x_{SME,i}(661) * m_{SME}(661)\right]}{\left[m_{heel}(660) + m_{SME}(661)\right]} \quad (4)$$

where $x_i(658)$, $x_i(657)$ and $x_{SME,i}(658)$ in Eq. (1) are the concentrations of species *i* (in weight fractions) in the MFT658, MFT657 and SME Batch 658 (SME658), respectively, and $m_{heel}(657)$ and $m_{SME}(658)$ are the mass of calcine solids in the MFT657 heel and the SME658 transferred, respectively. It is noted that $m_{SME}(657)$ to $m_{SME}(661)$ were calculated based on the measured calcine ratios of each SME batch; however, $m_{heel}(658)$ to $m_{heel}(660)$ were calculated using the calcine ratios of the respective heels which were calculated from measured calcine ratios of SME batches using similar mixing equations to Eq. (1) to Eq. (4).

5.1.2 Melt Pool

The derivation of the mixing model for the estimation of glass composition after successive multiple MFT batch feeding was given earlier and will not be repeated here.[5] It was shown that the concentration of species *i* in glass at the end of n^{th} MFT batch feeding, $\boldsymbol{x_{g,i}(t_n)}$, is calculated from Eq. (5):

$$x_{g,i}(t_n) = x_i(n) + \left[x_{g,i}(t_{n-1}) - x_i(n)\right] \exp[-N_n] \quad (5)$$

where $x_{g,i}(t_{n-1})$ = concentration of species *i* in glass at the end of $(n\text{-}1)^{th}$ MFT batch feeding, lb/lb
$x_i(n)$ = measured concentration of species *i* in n^{th} MFT batch, lb/lb calcine solids
N_n = number of melter turnovers during n^{th} MFT batch feeding

The rate of off-gas entrainment of species *i,* $\dot{m}_{e,i}$, is calculated from Eq. (6):

$$\dot{m}_{e,i} = \dot{m}_{cs}(n)x_{g,i}(t_n) - \dot{m}_g(k)x_{ps,i}(k) \quad (6)$$

where *k* = canister # being filled while the PS sample was taken.
$\dot{m}_{cs}(n)$ = average feed rate of n^{th} MFT batch during k^{th} canister filling, lb calcine solids/hr
$\dot{m}_g(k)$ = average glass pour rate during k^{th} canister filling, lb/hr
$x_{ps,i}(k)$ = measured concentration of species *i* in PS sample, lb/lb.

5.2 Case Study: SB7b

The SB7b PS sample was taken on 3/19/2013 at 10:28 hour while the MFT661 was being fed and Canister #4023 filled. The melter operating history and feed property data for the MFT661 and the four preceding batches, MFT657-660, are summarized in Table 1.[10-11] The melt pool was agitated with four bubblers at the total argon (Ar) flow rate of 4.7 scfm on average. It is particularly noted that the feeding was interrupted frequently while feeding MFT661 both before and after the PS sampling. For example, although the melter was first fed with the MFT661 five days earlier on 3/13/2013, the cumulative feeding time leading up the PS sampling was only ~19 hours due to frequent feeding difficulties which led to 13 feed pump restarts and 2 lengthy periods of idling each lasting 29 and 67 hours. As a result, the melter remained idling for ~75% of the time during the pre-PS sample MFT661. Furthermore, an estimated 50 gallons of pump prime water was added with each feed pump restart and it was estimated that the reported total solids of 35.2 wt% at the beginning of MFT661 decreased to ~30 wt% by the time of PS sampling based on the MFT slurry level data (LI3182). However, the uncertainties in any estimates based on LI3182 can be large as the slurry level readings fluctuated considerably due to repeated feed pump restarts. Thus, it was advised by the DWPF personnel that only the LI3182 data taken at the beginning and end of MFT661 be used in the mass balance but not the intermediate readings. For this reason, it was decided to take the entire MFT661 data into account in estimating the melt composition that was to be matched up against the measured PS composition in lieu of taking the MFT661 data only up to the time of PS sampling, as was done in previous studies.[4-5]

The total processing time for the five MFT batches considered was ~777 hours and the melter remained idling for ~139 hours, which is equivalent to 82% attainment. As noted above, the majority of that idling time occurred during MFT661, which led to 55 feed pump restarts. A total of 24 canisters were filled during MFT657-661, which is equivalent to 87,847 lb of glass poured. During the processing of MFT657-660, enough glass had been poured to achieve 5.2 melter turnovers and, based on the ideal mixing assumption, >99.5% of the glass remaining at the end of MFT656 would have been flushed out of the melter at the start of MFT661 (see Figure 3 in Ref. 4). This confirms that using the MFT657 calcined solid composition as the starting melt pool composition was a good approximation for predicting the melt pool composition at the time of SB7b PS sampling using Eq. (5).

The total solids (TS) and density data given in Table 1 are shown to decrease from the beginning to the end of each MFT batch as the MFT content was constantly diluted by the addition of both pump prime and trickle H_2O, the latter of which was assumed to be 20 gallons per day. Furthermore, as the content of every 5th MFT batch was sampled and analyzed for density, total solids and pH, it provided an opportunity to check the reported density and total solids in Table 1. Around the time of SB7b PS sampling, it was the MFT660 that was sampled; the measured density of 1.240 g/ml was practically identical to the reported value of 1.239 g/ml, while the measured TS was lower at 31.8 vs. the reported 33.7 wt%. As an accurate estimation of TS is just as important to the calcined solids balance, it was decided to derive a correlation between the density and TS from available MFT/SME data and use the resulting correlation to estimate TS from the reported density (ρ). Figure 2 shows the fit of the resulting correlation, Eq. (7), which was used to calculate the adjusted total solids given in Table 1:

$$TS = 132.3237 \ln(\rho) + 3.2199 \quad (7)$$

where TS is in weight percent (wt%) and ρ in g/ml. It is noted that the adjusted total solids are consistently lower than the reported values.

Table 1. Operating History and MFT Batch Bulk Properties for SB7b Mass Balance [10-11].

Batch	Beginning	Ending	Total Elapsed Time (hr)	Total Idling Time (hr)	# of Feed Pump Restart	MFT Level (gallon)	Max MFT Level (gallon)	Feed Factor (%)	Density (g/ml)	Reported Total Solids (wt%)	Adjusted Total Solids (wt%)	Glass Poured (lb)
657	2/22/2013 20:38	-	-	-	-	2,670	9,243	-	1.209	31.5	28.3	-
	-	2/28/2013 11:17	134.6	8.3	27	2,870	-	6.8	1.154	18.4	22.2	17,894
658	2/28/2013 15:55	-	-	-	-	6,018	9,656	-	1.206	29.0	28.0	-
	-	3/5/2013 06:28	110.5	1.8	12	3,529	-	12.6	1.180	23.0	25.1	15,083
659	3/5/2013 07:08	-	-	-	-	6,557	9,647	-	1.223	30.9	29.9	-
	-	3/9/2013 09:27	98.3	1.4	6	3,505	-	4.2	1.210	27.9	28.4	15,989
660	3/9/2013 09:28	-	-	-	-	3,505	9,181	-	1.239	33.7	31.6	-
	-	3/13/2013 11:27	98.0	0.7	3	3,140	-	11.9	1.232	30.1	30.8	17,501
661	3/13/2013 11:28	-	-	-	-	3,284	9,410	-	1.246	35.2	32.3	-
Pre-PS	-	3/18/2013 10:28	119.0	100.5	13	8,918	-	8.4	-	-	-	4,888
			PS sample taken while filling Can # 4023				Glass Density (g/ml) = 2.70			REDOX ($^{Fe2+}/Fe^{total}$) = 0.07		
661	3/18/2013 10:29	-	-	-	-	8,916	-	-	-	-	-	-
Post-PS	-	3/27/2013 05:09	210.7	20.7	42	2,305	-	22.8	1.125	10.8	18.8	16,491
661	3/13/2013 11:28	-	-	-	-	3,284	-	-	1.246	35.2	32.3	-
Total	-	3/27/2013 05:09	329.7	121.2	55	2,305	9,410	21.3	1.125	10.8	18.8	21,379
657-661	2/22/2013 20:38	3/27/2013 05:09	776.5	138.6	103	MFT Slurry Fed = 31,975 gallons		12.6	-	-	-	87,847

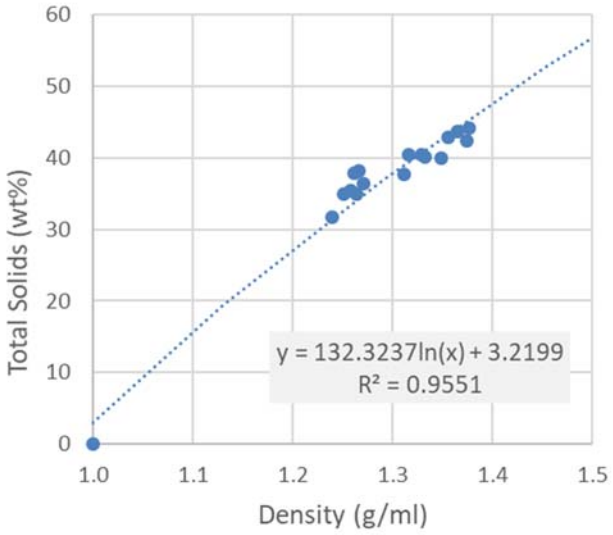

Figure 2. Measured Density vs. Total Solids of MFT/SME Samples of SB6, SB7a and SB7b.

5.2.1 Mass Balance Equations of SB7b

Eq. (5) was used to calculate the melt pool composition at the end of feeding each successive MFT batch using MFT657 as the starting melt pool composition as follows:

$$MELT658: \quad x_{g,i}(658) = x_i(658) + \left[x_{g,i}(657) - x_i(658)\right] \exp[-N_{658}] \tag{8}$$

$$MELT659: \quad x_{g,i}(659) = x_i(659) + \left[x_{g,i}(658) - x_i(659)\right] \exp[-N_{659}] \tag{9}$$

$$MELT660: \quad x_{g,i}(660) = x_i(660) + \left[x_{g,i}(659) - x_i(660)\right] \exp[-N_{660}] \tag{10}$$

$$MELT661: \quad x_{g,i}(661) = x_i(661) + \left[x_{g,i}(660) - x_i(661)\right] \exp[-N_{661}] \tag{11}$$

where $x_i(n)$ represents the composition of n^{th} MFT batch on a calcined solids basis and $x_{g,i}(n)$ the melt pool composition at the end of feeding n^{th} MFT batch. It is noted that both the melt pool composition and melter turnover of the last batch, $x_{g,i}(661)$ and N_{661}, are normally calculated up to the time of PS sampling; however, they were calculated by including the entire MFT661 due to large uncertainties in the LI3182 data stated above.

Finally, the rate of off-gas entrainment for species *i* was calculated as follows:

$$\dot{m}_{e,i} = \dot{m}_{cs}(661)x_{g,i}(661) - \dot{m}_g(661)x_{ps,i}(4023) \tag{12}$$

where $\dot{m}_{cs}(661)$ and $\dot{m}_g(661)$ are the time-averaged calcine solids feed and pour rates, respectively, over the duration of MFT661 and $x_{ps,i}(4023)$ is the measured concentration of species *i* in the PS glass sample taken while Canister #4023 was being filled. Except for the cold cap modeling, Eq. (12) was applied on an elemental basis rather than on an oxide basis.

5.2.2 Feed Chemistry of SB7b

This section describes the bases and assumptions made to develop the compositions of MFT658 - MFT661, i.e., $x_i(n)$'s in Eq. (1) to (4).

5.2.2.1 Charge Reconciliation of SME Product Data

The analytical data for the SB7b SME products is shown in Table 2; the elemental data is given on a wt% calcined solids (CS) basis, and the measured concentrations of NO_2^-, Cl^-, F^-, and PO_4^{3-} were all below detection limits. The charge imbalances that existed in the data were reconciled under the constraints of measured bulk properties such as total and calcined solids, pH, and density as well as the reported WL from the PCCS analysis. In doing so, the following bases and assumptions were applied:

1. All uranium (U) was assumed to be present as insoluble $Na_2U_2O_7$.
2. The remaining Na from Tank 40 after forming insoluble $Na_2U_2O_7$ was assumed to be soluble.
3. 80% of measured Ca and 60% of measured Mn were assumed to be soluble.
4. No sulfur was reported in the Inductively Coupled Plasma - Atomic Emission Spectroscopy (ICP-AES) data. As a result, the sulfur reported as SO_4^- by Ion Chromatography (IC) was assumed to represent 100% of sulfur in the SME samples, i.e., no insoluble sulfate.
5. The insoluble oxalate, calculated as the difference between the total and soluble oxalate by IC, was assumed to be present as CaC_2O_4.
6. All anion and elemental (except for Na) data was taken without any adjustments.

Assumptions #1 and #2 were necessary due to lack of analytical data for the SME product supernate phase. The Na data in Table 2 represents the total Na that came with both the sludge and the frit. The total Na was adjusted until the sum of negative charges of the anions were counterbalanced. The charge reconciliation results in Table 3 show that the measured Na concentrations had to be adjusted up by 10-23%, part of which could be attributed to Assumption #1; as the uranium, the 6th or 7th most abundant element in the feed, was assumed to form $U_2O_7^{2-}$ in lieu of UO_2^{2+}, it required as much as 5% of the Na in Tank 40 to be insoluble. This subsequently increased the soluble Na required for the charge reconciliation. Regardless, the total equivalent charge of anions was consistently greater than that of the cations for all five SME batches, even though the reported SME data was generally in line with the expected analytical uncertainty of ±10-15%. As a result, the total solids of the charge-reconciled SME products were all higher than the measured values by as much as 7.1%. As the concentration of carbonate (CO_3) was not measured, it was back calculated as the difference between the equivalent molar cation and anion concentrations after the adjustment of Na.

The percent insoluble Na, which consisted mostly of the frit Na and some diuranate precipitate ($Na_2U_2O_7$), was also calculated as part of the charge reconciliation. Table 3 shows that the SME660 that had the lowest reported WL of 31.43% had the highest percent insoluble Na at 36.3%, while the SME659 that had the highest WL of 34.22% had the lowest percent insoluble Na at 34.2%. These results were expected as the higher the WL, the less frit (thus insoluble Na) would be in the feed. Furthermore, the calculated WLs of the charge-reconciled SME products were lower than those from the PCCS analysis by 0.5-1.8% in absolute WL. It is also noted that the absolute difference between the PCCS and calculated WL was the smallest at 0.5% for the SME660 that had the greatest impact of all SME batches on the projected PS glass composition. The antifoam carbon remaining in the SME product was calculated as the difference between the measured total organic carbon (TOC) and the sum of formate and oxalate carbons. The resulting antifoam carbon concentrations remained relatively low at <1,000 ppm. The calcination ratio is defined as the fraction of calcined solids (CS) in the total solids (TS) or simply calculated as the mass or weight percent (wt%) ratio of CS to TS.

Table 2. Analytical Data Used in Charge Reconciliation of SME657-SME661.

Elements:	**SME657**	**SME658**	**SME659**	**SME660**	**SME661**
	(wt% CS)	(wt% CS)	(wt% CS)	(wt% CS)	(wt% CS)
Al	3.419	3.206	3.560	3.500	3.662
B	1.646	1.668	1.585	1.689	1.557
Ca	0.238	0.230	0.255	0.281	0.235
Cr	0.045	0.038	0.033	0.036	0.021
Cu	0.034	0.031	0.037	0.028	0.023
Fe	5.402	5.222	5.664	5.496	5.811
K	0.095	0.077	0.052	-0.058	-0.055
La	0.028	0.027	0.030	0.029	0.031
Li	2.581	2.612	2.517	2.554	2.430
Mg	0.116	0.111	0.123	0.113	0.127
Mn	1.153	1.090	1.226	1.138	1.235
Na	9.308	9.881	10.081	8.927	9.431
Ni	1.034	0.935	1.073	1.120	1.073
S	0.158	0.146	0.160	0.140	0.156
Si	25.388	25.299	24.118	26.578	25.483
Th	0.505	0.452	0.501	0.426	0.468
Ti	0.235	0.279	0.228	0.080	0.030
U	1.617	1.421	1.714	1.820	1.587
Zr	0.089	0.092	0.102	0.094	0.110
Anions:	(mg/kg)	(mg/kg)	(mg/kg)	(mg/kg)	(mg/kg)
NO_3	19,085	17,705	16,822	21,906	18,483
COOH	26,972	27,692	27,438	28,625	28,573
SO_4	1,409	1,304	1,504	1,373	1,512
C_2O_4	1,323	1,561	1,651	1,010	1,162
total C_2O_4	2,274	2,740	2,678	2,258	2,229
Misc.					
TOC (mg/kg)	8,145	8,451	8,938	8,613	8,738
Cs-137 (Bq/g)	5.25E+07	4.41E+07	4.70E+07	2.05E+07	2.83E+07
Density (g/ml)	1.251	1.265	1.271	1.312	1.267
Total Solids (wt%)	34.98	34.93	36.32	37.68	38.13
Calcined Solids (wt%)	30.26	29.93	31.03	33.59	32.51
Calcination Ratio	0.8650	0.8570	0.8543	0.8916	0.8525
PCCS Waste Loading (%)	32.55	32.26	34.22	31.43	33.59
pH	7.8	7.9	9.3	6.0	7.7

Table 3. Results of Charge Reconciliation of SME Product Analytical Data.

	SME657	SME658	SME659	SME660	SME661
Measured Na (wt% calcine)	9.31	9.88	10.08	8.93	9.43
Calculated Na (wt% calcine)	11.08	11.12	11.09	11.03	10.47
- % Na adjustment	19.0	12.5	10.0	23.5	11.0
Insoluble Na (% total Na)	35.70	35.88	34.24	36.35	35.22
Insoluble Na (% sludge Na)	4.2	3.7	4.3	4.8	4.3
Measured total solids (g/L)	437.5	441.7	461.4	494.2	483.0
Calculated total solids (g/L)	455.3	454.3	467.8	529.5	495.3
- Δ total solids (%)	4.1	2.8	3.4	7.1	2.6
PCCS WL (%)	32.55	32.26	34.22	31.43	33.59
Calculated WL (%)	31.31	30.48	33.12	30.91	31.74
- Δ from PCCS WL (%)	-1.24	-1.78	-1.10	-0.52	-1.85
Calculated antifoam carbon (mg/kg)	244	129	816	359	579
Calculated Ca as oxalate (% total Ca)	76.0	97.7	73.4	77.3	80.0
Calculated CO_3 (g/L)	0.022	0.025	3.254	0	0.022

The charge-reconciled compositions of SME657 to SME661 are given in Table 4 on an elemental wt% CS basis. It is noted that the concentrations of those elements with an asterisk (*), notably the noble metals and Tc-99, were measured in the PS sample but not in the SME samples. Thus, to facilitate the off-gas carryover projections of those minor or trace-level species, their concentrations in the SME product were estimated using their respective ratios to Fe in Tank 40, which is in principle a reasonable approximation as they were neither added nor removed and remained nonvolatile during the SRAT/SME processing. The concentrations of those "ratio-projected" species are shown in blue numbers and were 3 to 4 orders-of-magnitude lower than the dominant Si. The concentration of K in the SME660 and SME661 is shown as zero as their reported values in Table 2 were negative. The concentrations of all measured species summed to within 100±3 wt% on an oxide basis, which indicates the overall consistency of the ICP-AES data.

Also shown in Table 4 is the composition of Tank 40 on a wt% total solids (TS) basis.[12] Although Hg and Nd were measured at 1.71 and 0.251 wt%, respectively, they were excluded as they were not detected in the PS sample; however, they are still included in the total solids. On the other hand, the concentration of B in Tank 40 was below detection limits but still included as B_2O_3 is one of the major oxides in the DWPF glass. Because of the unit differences, a direct comparison between Tank 40 and SME compositions cannot be made; but their relative concentrations with respect to Fe can be compared, as shown in Table 5. It is clearly seen that the largest increase in concentration from Tank 40 to the SME occurred to B, Li, and Si as a result of frit addition; the increase in Si was ~1/4 that of B or Li because its concentration in Tank 40 was ~2 orders of magnitude higher than B and Li. Despite being a frit component, the increase in the relative concentration of Na was not nearly as large because ~2/3 of the measured Na originated from Tank 40. The relative concentrations of Ti and Cs-137 also increased significantly due to the inputs from the Actinides Removal Process (ARP) and the Modular CSSX Unit (MCU), respectively, as shown in Figure 1. The concentration of K in the charge-reconciled SME660 and SME661 was negative, which is why its relative concentration changed by -100%. The calculated percent increases or decreases of the minor or trace-level species such as Cr, Cu and K should be considered rough estimates as the analytical uncertainties could potentially lead to questionable results. The potential sources for the excess Cr and Cu are discussed later in the report. It is noted that the relative concentrations of those species with an (*) remained unchanged since their SME concentrations were estimated using their respective ratios to Fe in Tank 40.

Table 4. Charge-Reconciled Elemental Compositions of SME657-SME661 vs. Tank 40.

Elements:	Tank 40	SME657	SME658	SME659	SME660	SME661
	(wt% TS)	(wt% CS)	(wt% CS)	(wt% CS)	(wt% CS)	(wt% CS)
Al	9.18	3.376	3.203	3.588	3.411	3.634
B	<0.016	1.625	1.667	1.598	1.646	1.545
Ba*	0.0979	0.038	0.037	0.040	0.038	0.041
Ca	0.699	0.235	0.230	0.257	0.274	0.233
Cd	0.0288	0.011	0.011	0.012	0.011	0.012
Ce	0.135	0.052	0.051	0.055	0.052	0.056
Co*	0.0135	0.005	0.005	0.006	0.005	0.006
Cr	0.0405	0.044	0.038	0.033	0.035	0.021
Cu	0.0437	0.033	0.031	0.038	0.027	0.022
Fe	13.9	5.335	5.218	5.710	5.356	5.768
Gd*	0.074	0.028	0.028	0.030	0.028	0.031
K	0.054	0.093	0.077	0.053	0.000	0.000
La*	0.073	0.028	0.027	0.030	0.028	0.030
Li	0.0247	2.548	2.610	2.537	2.489	2.412
Mg	0.296	0.115	0.111	0.124	0.110	0.126
Mn	3.09	1.138	1.089	1.235	1.109	1.226
Na	14.4	10.865	11.028	11.096	10.672	10.312
Ni	2.69	1.021	0.934	1.082	1.092	1.065
P*	0.115	0.044	0.043	0.047	0.044	0.048
Pb*	0.0261	0.010	0.010	0.011	0.010	0.011
Pd*	0.00254	0.001	0.001	0.001	0.001	0.001
Ag*	0.0118	0.005	0.004	0.005	0.005	0.005
Rh*	0.0207	0.008	0.008	0.009	0.008	0.009
Ru*	0.102	0.039	0.038	0.042	0.039	0.042
S	0.49	0.156	0.146	0.162	0.136	0.155
Si	1.11	25.091	25.292	24.377	25.299	25.338
Sr*	0.0443	0.017	0.017	0.018	0.017	0.018
Th	1.08	0.499	0.452	0.505	0.415	0.464
Ti	0.0181	0.232	0.278	0.229	0.078	0.030
U	4.78	1.596	1.420	1.727	1.774	1.575
Zn*	0.0396	0.015	0.015	0.016	0.015	0.016
Zr	0.176	0.088	0.092	0.103	0.091	0.109
Cs-137	7.41E-04	1.62E-03	1.37E-03	1.48E-03	6.22E-04	8.76E-04
Tc-99*	5.70E-04	2.19E-04	2.14E-04	2.34E-04	2.20E-04	2.37E-04
Total	54.968	54.395	54.228	54.828	54.413	54.467
Total - Ratioed	-	54.054	53.894	54.463	54.070	54.097
Total - Ratioed (oxide)	-	101.321	100.155	99.174	102.647	100.760

* Indicates species whose SME concentrations (in blue) were estimated using their respective ratios to Fe in Tank 40.

Table 5. Changes in Relative Concentrations with Respect to Fe from Tank 40 to SME.

Elements	Tank 40	SME657	SME658	SME659	SME660	SME661
	(ratio to Fe)	Δ Fe ratio (%)	Δ Fe ratio (%)	Δ Fe ratio (%)	Δ Fe ratio (%)	Δ Fe ratio (%)
Al	0.660	-4	-7	-5	-4	-5
B	<0.001	26,366	27,654	24,213	26,598	23,177
Ba*	0.007	0	0	0	0	0
Ca	0.050	-12	-13	-11	2	-20
Cd*	0.002	0	0	0	0	0
Ce*	0.010	0	0	0	0	0
Co*	0.001	0	0	0	0	0
Cr	0.003	183	150	98	123	24
Cu	0.003	97	87	110	61	23
Fe	1.000	0	0	0	0	0
Gd*	0.005	0	0	0	0	0
K	0.004	354	284	139	-100	-100
La*	0.005	0	0	0	0	0
Li	0.002	26,781	28,050	24,907	26,050	23,429
Mg	0.021	1	0	2	-4	3
Mn	0.222	-4	-6	-3	-7	-4
Na	1.036	97	104	88	92	73
Ni	0.194	-1	-8	-2	5	-5
P*	0.008	0	0	0	0	0
Pb*	0.002	0	0	0	0	0
Pd*	0.000	0	0	0	0	0
Ag*	0.001	0	0	0	0	0
Rh*	0.001	0	0	0	0	0
Ru*	0.007	0	0	0	0	0
S	0.035	-17	-21	-20	-28	-24
Si	0.080	5,790	5,970	5,246	5,815	5,401
Sr*	0.003	0	0	0	0	0
Th	0.078	20	11	14	0	4
Ti	0.001	3,241	3,998	2,984	1,020	294
U	0.344	-13	-21	-12	-4	-21
Zn*	0.003	0	0	0	0	0
Zr	0.013	30	39	43	35	49
Cs-137	5.33E-05	468	394	385	118	185
Tc-99*	4.10E-05	0	0	0	0	0

* Species whose SME concentrations were estimated based on their respective ratios to Fe in Tank 40.

5.2.2.2 Calculation of MFT Batch Composition

Once the SME product is transferred to the MFT, it is blended with the heel and continuously diluted with both pump prime and trickle water flows until it is fed to the melter. This means that once the composition of calcine solids in each MFT batch is calculated from Eq. (1) - Eq. (4) using the amounts of calcine solids remaining in the heel and that in the next SME transfer, e.g., $m_{heel}(657)$ and $m_{SME}(658)$, respectively, it will remain the same until the next SME batch is transferred to the MFT. The calcine ratio, which is defined as the ratio of calcine solids (or oxides) to total solids, of the new MFT batch was also calculated by mass-averaging the calcine ratios of the heel and the SME transfer. However, as the density and total solids both vary with dilution, they need to be measured or estimated accurately for the successful determination of calcine solids fed to the melter using the MFT slurry level data (LI3182). Unlike the SME batches, the content of each MFT batch is not analyzed for the full elemental and ionic compositions. Instead, every 5th MFT batch is analyzed for the total solids, density and pH, which gave an opportunity to check the accuracy of the reported total solids and density at the beginning of MFT660 against the measured data. As stated in Section 5.2, the reported density of 1.239 g/ml was essentially identical to the measured value of 1.240 g/ml, while the estimated total solids were off. For this reason, the reported density data was taken as accurate and the total solids were estimated from the reported density using Eq. (7).

The calcined solids in the heel and SME transfer were calculated using the MFT volume (LI3182), density and adjusted total solids from Table 1. For example, the calcined solids in the MFT657 heel was calculated from the remaining volume of 2,870 gallons along with the density and total solids at the end of MFT657:

$$m_{heel}(657) = \frac{(2{,}870\ gal)\left(3{,}785.4\ \frac{ml}{gal}\right)\left(1.154\ \frac{g}{ml}\right)(0.2217)\left(0.865\ \frac{g\ CS}{g\ TS}\right)}{453.6\ \frac{g}{lb}}$$

$$= 5{,}301\ lb \quad (13)$$

The calcined solids in the SME658 transfer was calculated from the volume increase at the end of transfer, i.e., V_{max} - $V_{initial}$ = 9,656 – 2,870 = 6,786 gallons along with the initial density and total solids of MFT658:

$$m_{SME}(658) = \frac{(6{,}786\ gal)\left(3{,}785.4\ \frac{ml}{gal}\right)\left(1.206\ \frac{g}{ml}\right)(0.28)\left(0.857\ \frac{g\ CS}{g\ TS}\right)}{453.6\ \frac{g}{lb}}$$

$$= 16{,}391\ lb \quad (14)$$

The sum of $m_{heel}(657)$ and $m_{SME}(658)$ constituted the total calcine solids in MFT658. It is noted that the calcination ratio 0.865 used in Eq. (13) for $m_{heel}(657)$ was the same as that of SME657 in Table 2 because SME657 was set as the first batch. The calcination ratios of the subsequent heels were equal to those of the same MFT batches which were in turn calculated by mass averaging the calcination ratios of the heel of the previous batch and the SME transfer. For example, the calcination ratio of the MFT658 was calculated as:

$$CR_{MFT}(658) = \frac{m_{SME}(658)CR_{SME}(658) + m_{heel}(657)CR_{heel}(657)}{m_{SME}(658) + m_{heel}(657)}$$

$$= \frac{(16{,}391)(0.857) + (5{,}301)(0.865)}{16{,}391 + 5{,}301}$$

$$= 0.8589 \quad (15)$$

The calcined solids and calcination ratios calculated per Eq. (13) – Eq. (15) are tabulated in Table 6. The impact of heels can be gleaned from the calculated calcination ratios being different from those of the SME products given in Table 2, especially for the MFT660. Also shown are the calculated insoluble Na fractions in each MFT batch ranging from 0.3475 to 0.3583; a small but non-zero effect of heels can be seen when they are compared to those of the SME batches in Table 3. The fractions of B, Li and Si that originated from the frit addition were calculated to be 100%, 99.6% and 98.3% of their respective totals.

Table 6. Calcined Solids and Calcination Ratios of MFT657-MFT661.

	MFT657	MFT658	MFT659	MFT660	MFT661
SME Transfer (lb)	22,855	16,391	15,929	16,615	17,965
MFT Heel (lb)	0	5,301	7,498	8,616	8,753
Total (lb)	22,855	21,691	23,427	25,232	26,717
Calcination Ratio (%)	86.50	85.89	85.58	87.94	86.13
Insoluble Na (% total Na)	35.70	35.83	34.75	35.80	35.41

The calculated elemental compositions of MFT657 to MFT661 using the parameters in Table 6 are shown in Table 7 on a wt% CS basis. These MFT compositions represent $x_i(n)$ in Eqs. (1) to (4); the composition of MFT657 or $x_i(657)$ is the same as that of SME657 in Table 4. The concentrations in blue numbers represent those species whose SME concentrations were estimated by fixing the concentration ratios with respect to Fe at their respective ratios in Tank 40.[12] The sum of the measured oxides was within 100±0.4%, regardless of whether those elements with an asterisk were included or not, which gives credence to the SME analytical data used in the charge reconciliation and the approach taken to estimate the SME concentrations of those minor or trace-level species not measured using their ratios to Fe in Tank 40.

Table 7. Calculated Elemental Compositions of MFT657-MFT661 Including Heels.

Elements:	MFT657	MFT658	MFT659	MFT660	MFT661
	(wt% CS)	(wt% CS)	(wt% CS)	(wt% CS)	(wt% CS)
Al	3.376	3.245	3.479	3.434	3.569
B	1.625	1.657	1.617	1.636	1.575
Ba*	0.038	0.037	0.039	0.038	0.040
Ca	0.235	0.231	0.248	0.265	0.244
Cd	0.011	0.011	0.012	0.011	0.012
Ce	0.052	0.051	0.054	0.053	0.055
Co*	0.005	0.005	0.005	0.005	0.005
Cr	0.044	0.039	0.035	0.035	0.025
Cu	0.033	0.031	0.036	0.030	0.025
Fe	5.335	5.247	5.562	5.426	5.656
Gd*	0.028	0.028	0.029	0.029	0.030
La*	0.028	0.028	0.029	0.028	0.030
Li	2.548	2.595	2.556	2.512	2.444
Mg	0.115	0.112	0.120	0.113	0.122
Mn	1.138	1.101	1.192	1.137	1.197
Na	10.865	10.988	11.062	10.805	10.474
Ni	1.021	0.955	1.041	1.074	1.068
P*	0.044	0.043	0.046	0.045	0.047
Pb*	0.010	0.010	0.010	0.010	0.011
Pd*	0.001	0.001	0.001	0.001	0.001
Ag*	0.005	0.004	0.005	0.005	0.005
Rh*	0.008	0.008	0.008	0.008	0.008
Ru*	0.039	0.039	0.041	0.040	0.042
S	0.156	0.148	0.157	0.144	0.151
Si	25.091	25.243	24.654	25.079	25.253
Sr*	0.017	0.017	0.018	0.017	0.018
Th	0.499	0.463	0.492	0.441	0.457
Ti	0.232	0.267	0.241	0.134	0.064
U	1.596	1.463	1.643	1.729	1.625
Zn*	0.015	0.015	0.016	0.015	0.016
Zr	0.088	0.091	0.099	0.094	0.104
Cs-137	1.62E-03	1.43E-03	1.46E-03	9.09E-04	8.87E-04
Tc-99*	2.19E-04	2.15E-04	2.28E-04	2.23E-04	2.32E-04
Total	54.395	54.269	54.649	54.494	54.475
Total - Ratioed	54.054	53.933	54.293	54.147	54.114
Total – Ratioed (oxides)	99.786	99.803	99.820	99.872	99.884

* Species whose SME concentrations were estimated based on their respective ratios to Fe in Tank 40.

5.2.3 Mass Balance Calculations of SB7b

This section describes the bases and assumptions used to calculate the melt pool compositions from the MFT compositions given in Table 7 and subsequent off-gas carryover projections of some of the key species.

5.2.3.1 Bases and Assumptions

Table 8 lists the values of key operating parameters used to calculate the melt compositions using Eq. (8) to Eq. (11) and the off-gas entrainment rates using Eq. (12). The key bases and assumptions used, including those discussed earlier, are highlighted next:

1. Available analytical data for the SB7b PS glass sample taken on 3/19/2013 at 10:28 while MFT661 was being fed and Can #4023 being filled constituted the glass composition, $x_{PS,i}(4023)$, against which the predicted glass composition, $x_{g,i}(661)$, was compared.[13]

2. Frequent feed interruptions produced inconsistent MFT level data (LI3182) throughout the duration of MFT661 feeding except at the start and finish. As a result, the melt pool composition at the time of PS glass sampling was assumed to be that calculated using the data taken at the end of MFT661.

3. Inclusion of four preceding batches, MFT657-MFT660, provided enough feed material to produce 5.22 melter turnovers, at which >99% of the pre-MFT657 melt pool composition would have been flushed out. This justified the assumption of making the composition of MFT657 given in Table 7 the initial melt pool composition, i.e., $x_i(657) = x_{g,i}(657)$.

4. It was assumed that it would take 2 hours for the fresh feed material to become calcined and melted. Thus, the melter turnover for MFT661 (N_{661}) was reduced by the calcination time of 2 hours.

Table 8. Operating Parameters and MFT580 Properties for SB7a Mass Balance Calculations.

Parameters	Value
Melter turnover:	
- N_{657}	1.36
- N_{658}	1.23
- N_{659}	1.27
- N_{660}	1.36
- N_{661}	1.67
Mass flow rate:	
- $\dot{m}_{cs}(661)$ (lb/hr)	104.9
- $\dot{m}_{g}(661)$ (lb/hr)	102.5
Can #4023 filling cycle (hr)	26.0
MELT661:	
- calcination time (hr)	2.00
- glass density (g/ml)[6]	2.7
- REDOX	0.07

The melter turnover during the nth MFT batch feeding (N_n) was calculated as:

$$N_n = \frac{m_{CS\_fed}(n)}{m_{melt\_pool}(n)} \quad (16)$$

where $m_{CS\_fed}(n)$ is the total calcined solids fed during the n[th] MFT batch feeding and $m_{melt\_pool}(n)$ is the total glass in the melt pool at the average melt depth (LI3523). For example, the total MFT(661) calcined solids fed was 21,876 lb and the total glass in the melter at the average melt depth of 32.62 inches was 12,955 lb or 396 lb glass/inch. Thus, N_{661} = 21,876/12,955 = 1.69, which is further reduced to 1.67, as shown in Table 8, after subtracting the 2-hour calcination time from the total feeding time. It is noted that $m_{CS\_fed}(661)$ of 21,876 lb is less than the total calcined solids in MFT661 of 26,717 lb in Table 6 as the latter also included $m_{heel}(661)$ which was blended with the next SME transfer, $m_{SME}(662)$.

5.2.3.2 Calculation Steps

The mass balance calculations proceeded as follows:

1. Set $x_{g,i}(657)$ = concentration of species *i* in the "MFT657" column of Table 7.
2. Set $x_i(658)$ = concentration of species *i* in the "MFT658" column of Table 7.
3. Substitute $x_{g,i}(657)$ and $x_i(658)$ along with N_{658} from Table 8 into Eq. (8) and solve for $x_{g,i}(658)$.
4. Set $x_i(659)$ = concentration of species *i* in the "MFT659" column of Table 7.
5. Substitute $x_{g,i}(658)$ and $x_i(659)$ along with N_{659} from Table 8 into Eq. (9) and solve for $x_{g,i}(659)$.
6. Calculate $x_{g,i}(660)$ and $x_{g,i}(661)$ from Eq. (10) and (11), respectively. by repeating Step 4 and 5.
7. Set $x_{ps,i}(4023)$ = concentration of species *i* in the "PS Glass" column of Table 9.
8. Substitute $x_{g,i}(661)$, $x_{ps,i}(4023)$ and the calcined feed and glass pour rates, $\dot{m}_{cs}(661)$ and $\dot{m}_g(661)$ from Table 8 into Eq. (12) and calculate the off-gas entrainment rate of species *i*, $\dot{m}_{e,i}$.

5.2.4 Results of SB7b Mass Balance

The melt composition at the time of PS sampling denoted by MELT661 was calculated and compared with the measured PS sample composition. The off-gas carryover projections were then made using the overall mass balance Eq. (12) for all measured as well as ratio-projected species, including the radionuclides.

5.2.4.1 Calculated Melt vs. PS Sample Compositions

The MFT compositions in Table 7 were input into Eq. (8) to Eq. (11) to calculate the melt compositions at the end of feeding MFT658 to MFT661, respectively. The resulting melt compositions are compared to the measured PS sample composition in Table 9.[13] Focusing only on the major species of concentrations >1%, the MELT661 vs. PS sample comparison in Table 10 shows a clear bias; the predicted concentrations of the frit components (B, Li and Si) in MELT661 were 8-10% higher than their counterparts in the PS sample (or 9.1% collectively), while the concentrations of the sludge components (Al, Fe, Mn, Ni and U) were 2-24% lower (or -10.7% collectively). When the reported total U was replaced with the sum of its isotopes ($\Sigma U_{isotope}$), whose concentrations were calculated based on their respective ratios to Fe in Tank 40, the concentrations of the sludge components were 2-13% lower than their counterparts in the PS sample (or -8.9% collectively). Thus, the predicted concentrations of the frit and sludge components were collectively off from their respective PS sample counterparts essentially by the same extent but in the opposite direction: +9 vs. -9% rounded to the nearest percent.

Table 9. Calculated Elemental Compositions of MELT657-MELT661 vs. PS Sample.

Elements:	MELT657	MELT658	MELT659	MELT660	MELT661	PS Sample
	(wt%)	(wt%)	(wt%)	(wt%)	(wt%)	(wt%)
Al	3.376	3.284	3.424	3.432	3.543	4.010
B	1.625	1.648	1.625	1.633	1.586	1.465
Ba*	0.038	0.037	0.039	0.038	0.040	0.045
Ca	0.235	0.232	0.244	0.260	0.247	0.311
Cd*	0.011	0.011	0.011	0.011	0.012	0.013
Ce*	0.052	0.051	0.053	0.053	0.055	0.063
Co*	0.005	0.005	0.005	0.005	0.005	0.006
Cr	0.044	0.041	0.037	0.035	0.027	0.055
Cu	0.033	0.032	0.035	0.031	0.026	0.156
Fe	5.335	5.272	5.481	5.440	5.615	6.068
Gd*	0.028	0.028	0.029	0.029	0.030	0.037
La*	0.028	0.028	0.029	0.029	0.029	0.036
Li	2.548	2.581	2.563	2.525	2.459	2.245
Mg	0.115	0.113	0.118	0.115	0.121	0.130
Mn	1.138	1.112	1.170	1.146	1.187	1.283
Na	10.865	10.952	11.031	10.863	10.547	10.700
Ni	1.021	0.974	1.022	1.061	1.067	1.085
P*	0.044	0.044	0.045	0.045	0.046	0.065
Pb*	0.010	0.010	0.010	0.010	0.011	0.018
Pd*	0.001	0.001	0.001	0.001	0.001	0.001
Ag*	0.005	0.004	0.005	0.005	0.005	0.012
Rh*	0.008	0.008	0.008	0.008	0.008	0.007
Ru*	0.039	0.039	0.040	0.040	0.041	0.021
S	0.156	0.150	0.155	0.147	0.151	0.161
Si	25.091	25.198	24.806	25.009	25.207	23.100
Sr*	0.017	0.017	0.017	0.017	0.018	0.019
Th	0.499	0.474	0.487	0.453	0.456	0.462
Ti	0.232	0.257	0.246	0.163	0.082	0.153
U	1.596	1.502	1.603	1.697	1.639	2.168
Zn*	0.015	0.015	0.016	0.015	0.016	0.042
Zr	0.088	0.090	0.097	0.095	0.102	0.064
Cs-137	1.62E-03	1.49E-03	1.47E-03	1.05E-03	9.18E-04	9.13E-04
Tc-99*	2.19E-04	2.16E-04	2.25E-04	2.23E-04	2.30E-04	4.19E-05
Total	54.395	54.306	54.553	54.509	54.482	53.955
Total - Ratioed	54.054	53.969	54.202	54.161	54.122	53.955
Total – Ratioed (oxides)	99.786	99.798	99.814	99.857	99.879	97.906
Insoluble Na (% total Na)	35.7%	35.8%	35.0%	35.6%	35.4%	35.4%

* Species whose SME concentrations were estimated based on their respective ratios to Fe in Tank 40.

Table 10. Predicted vs. Measured SB7b Glass compositions and Off-Gas Carryover Rates.

Element:	MELT 661	PS Sample	Δ (MELT661-PS Sample)	Off-Gas Carryover	Adjusted PS Sample	Adjusted Off-Gas Carryover
	(wt%)	(wt%)	(% PS)	(% fed)	(wt%)	(% fed)
Al	3.543	4.010	-12%	-12.9%	3.541	2.3%
B	1.586	1.465	8%	7.9%	1.602	1.3%
Ba*	0.040	0.045	-11%	-12.4%	0.039	2.7%
Ca	0.247	0.311	-21%	-25.7%	0.274	-8.8%
Cd*	0.012	0.013	-13%	-14.7%	0.012	0.8%
Ce*	0.055	0.063	-13%	-14.5%	0.055	0.9%
Co*	0.005	0.006	-11%	-11.5%	0.005	3.5%
Cr	0.027	0.055	-51%	-102.1%	0.049	-74.8%
Cu	0.026	0.156	-83%	-496.6%	0.138	-416.2%
Fe	5.615	6.068	-7%	-7.8%	5.358	6.8%
Li	2.459	2.245	10%	9.0%	2.455	2.5%
Mg	0.121	0.130	-7%	-7.3%	0.115	7.1%
Mn	1.187	1.283	-7%	-7.7%	1.132	6.8%
Na	10.547	10.700	-1%	-1.2%	10.246	5.1%
Ni	1.067	1.085	-2%	-1.5%	0.958	12.2%
S	0.151	0.161	-6%	-6.3%	0.142	8.0%
Si	25.207	23.100	9%	8.6%	25.257	2.1%
Sr*	0.018	0.019	-7%	-7.4%	0.017	7.1%
Th	0.456	0.462	-1%	-1.1%	0.408	12.5%
Th-232*	0.436	0.487	-10%	-11.2%	0.430	3.8%
Ti	0.082	0.153	-46%	-85.1%	0.135	-60.1%
U	1.639	2.168	-24%	-31.9%	1.914	-14.1%
$\Sigma U_{isotope}$*	1.931	2.208	-13%	-14.0%	1.949	1.3%
Zr	0.102	0.064	59%	37.2%	0.057	45.7%
Total (U/Th)	54.481	54.441			54.510	
Total ($\Sigma U_{isotope}$/Th-232)	54.753	54.482			54.546	
Total (U/Th) - Ratioed	54.122	54.441			54.510	
Total ($\Sigma U_{isotope}$/Th-232) - Ratioed	54.394	54.482			54.546	
Total - Ratioed (oxides)	99.879	97.906			99.932	
Total ($\Sigma U_{isotope}$/Th-232) - Ratioed (oxides)	100.202	97.953			99.974	
B+Li+Si	29.253	26.810	9.1%	8.6%	29.313	2.1%
Al+Fe+Mn+Ni+U	13.051	14.613	-10.7%	-11.7%	12.903	3.4%
Al+Fe+Mn+Ni+$\Sigma U_{isotope}$	13.344	14.653	-8.9%	-9.5%	12.939	5.2%

* Species whose SME concentrations were estimated based on their respective ratios to Fe in Tank 40.

5.2.4.2 Off-Gas Carryover Rates and Adjustment of PS Sample Composition

It is also noted in Table 10 that the predicted Na concentration in the MELT661 was lower only by 1% than its PS sample counterpart –thus, they were essentially the same. Being made up of approximately 36% frit Na and 64% sludge Na, the negligible difference between the predicted and measured total Na was expected from the equal but opposite deviations exhibited by the sludge and frit groups. All this indicates that the calculated off-gas carryover rates of B, Li and Si using Eq. (12) ranged from 7.9 to 9% fed (or 8.6% collectively), while those of the sludge components ranged from -1.5 to -31.9% fed (or -11.7% collectively). When U was replaced with $\Sigma U_{isotope}$, the upper bound of the negative sludge carryover rates decreased from -31.9 to -14% and the collective (or overall) carryover rate decreased from -11.7 to -9.5%. While the large negative off-gas carryover rates of most sludge components are not physically feasible, the nearly equal but opposite overall carryover rates of the frit and sludge groups (i.e., 8.6% and -9.5%, respectively) are the result of the PS sample being low in frit compared to the MELT661. As a result, the calculated WL of the PS sample was high at 36.8% vs. 31.6% for the MELT661 and the large WL discrepancy was resolved in this study by assuming that the measured PS sample composition was biased low in frit (or biased high in sludge), which meant that the predicted WL of MELT661 was taken to be representative of the PS sample. Some support for this premise comes from the fact that the MELT661 WL was calculated based on those of individual SME batches which were in turn determined from the PCCS analysis as part of the DWPF process controls.

Another way to reconcile the large WL difference between the projected and measured glass compositions would be to override the PCCS WLs of all five SME batches and vary them simultaneously until the calculated WL of MELT661 equals that of the PS sample, 36.8%. Since the PCCS WLs were set based on the fixed sludge oxides/Fe ratio of 5.75 for SB7b, they can be adjusted by changing either the sludge oxides loading in Tank 40 or the Fe concentration in the SME. Since Fe is the third most abundant species after Si and Na in the SME, it would be difficult to justify adjusting it alone and, even then, it must be adjusted for all five SME batches as its measured concentrations remained relatively steady, as shown in Table 7. It means that adjusting the Fe concentrations would be more arbitrary and thus more difficult than adjusting the PS sample composition and, not to mention, it requires that charge reconciliation be redone. The other option of adjusting the sludge oxides loading would be simpler but it would mean overriding the results of the Tank 40 Waste Acceptance Preliminary Specifications (WAPS) sample analysis. Regardless, since the off-gas carryover rate of each element was calculated as the difference between its feed and glass pour rates, adjusting the PCCS WLs (and thus the feed composition) vs. adjusting the PS sample composition would likely produce similar carryover results at the given overall feed and glass pour rates.

Thus, the measured concentrations of B, Li and Si in the PS sample were adjusted up by the same percentage iteratively until the WL of the adjusted and renormalized PS sample composition equaled that of MELT661. It turned out that the reported concentrations of B, Li and Si in the PS glass had to be adjusted up by 24% to match the MELT661 WL and the pre- and post-adjustment PS glass compositions are compared to that of MELT661 in Table 10 along with the resulting off-gas carryover projections. The equivalent results for the reported radionuclides are shown in Table 11; the concentrations of all radionuclides except Cs-137 were calculated based on their respective ratios to Fe in Tank 40.[14] Several significant improvements can be seen in the post-adjustment off-gas carryover rates of both the frit and sludge components. For example, the large positive carryover rates of the frit components (before adjustment) remained positive but became smaller after the adjustment, ranging from 1.3% (B) to 2.5% (Li) with the overall carryover rate of frit decreasing from 8.6% to 2.1%, which is closer to the DWPF design basis entrainment rate of 1% for non-bubbled melter operation.[15] It is noted that the Measurement Acceptability Region (MAR) assessment was performed on the adjusted PS glass composition, and the results showed that it met all DWPF glass product constraints except for the sulfate limit, which is controlled administratively due to its conservatively-low MAR limit.[16] The sulfate concentration in both the measured and adjusted SB7b PS sample was confirmed to be below the Na_2SO_4 solubility limit of 0.88 wt% with Frit 418, which was developed by the SRNL.[32]

Likewise, the large negative carryover rates of the major sludge components at concentrations >1% became positive (except U) and, as a result, the overall carryover rate of the sludge group (Al, Fe, Mn, Ni and U) changed from -11.7% to 3.4% after the adjustment. The carryover rate of U remained large and negative at -14.1% but that of $\Sigma U_{isotope}$ was positive at +1.3%, close to the DWPF design basis, which gives credence to the approach taken, i.e., estimating the SME concentrations of those not measured using their respective ratios to Fe in Tank 40, including the radionuclides. As expected, however, the positive carryover rate of $\Sigma U_{isotope}$ pushed the overall carryover rate of the sludge group higher from 3.4% to 5.2%; either overall carryover rate seems high mainly because that of Fe, which is the most dominant sludge species, was quite high at 6.8%. Considering that the standard deviation of Fe concentrations in the MELT657 to MELT661 in Table 9 was only 2% of the mean before it increased to 11% when the PS sample was included, it may be speculated that the concentration of Fe in the PS glass also could have been reported low, as the oxides of the measured PS glass components summed up to 97.9% vs. 99.8% or higher for the MELTs.

Table 11. Predicted vs. Measured SB7b Glass Isotopic Compositions and Off-Gas Carryover Rates.

Isotope:	MELT 661	PS Sample	Δ (MELT661-PS Sample)	Off-Gas Carryover	Adjusted PS Sample	Adjusted Off-Gas Carryover
	(wt%)	(wt%)	(% PS)	(% fed)	(wt%)	(% fed)
Sr-90*	3.76E-03	3.42E-03	10%	9.3%	3.02E-03	21.5%
Zr-93*	7.43E-03	6.38E-03	17%	14.4%	5.63E-03	26.0%
Tc-99*	2.30E-04	4.19E-05	450%	81.9%	3.70E-05	84.3%
Cs-137	9.18E-04	9.13E-04	1%	0.8%	8.06E-04	14.2%
Th-232*	4.36E-01	4.87E-01	-10%	-11.2%	4.30E-01	3.8%
U-233*	1.76E-04	<3.89E-04	-	-	-	-
U-234*	2.62E-04	<3.89E-04	-	-	-	-
U-235*	1.14E-02	1.21E-02	-6%	-5.8%	1.07E-02	8.5%
U-236*	5.66E-04	5.81E-04	-3%	-2.4%	5.13E-04	11.4%
U-238*	1.92E+00	2.20E+00	-13%	-14.1%	1.94E+00	1.3%
Np-237*	1.41E-03	1.54E-03	-8%	-8.9%	1.36E-03	5.7%
Pu-238*	3.36E-04	3.16E-04	6%	6.1%	2.79E-04	18.8%
Pu-239*	6.99E-03	8.55E-03	-18%	-21.9%	7.55E-03	-5.5%
Pu-240*	6.34E-04	7.96E-04	-20%	-25.1%	7.03E-04	-8.3%
Pu-241*	2.00E-05	1.71E-05	17%	14.6%	1.51E-05	26.1%
Pu-242*	<9.49E-05	<3.89E-04	-	-	-	-
Am-241*	4.20E-04	4.40E-04	-5%	-4.6%	3.89E-04	9.5%
Total	2.39E+00	2.72E+00			2.40E+00	
$\Sigma U_{isotope}$	1.93E+00	2.21E+00			1.95E+00	1.3%
$\Sigma U_{isotope}$+Th	2.37E+00	2.69E+00			2.38E+00	
$\Sigma U_{isotope}$+Th (% total)	99.1%	99.2%			99.2%	

* Isotopes whose SME concentrations were estimated using their respective ratios to Fe in Tank 40.

As was the case with U, the concentration of Th in the SME was also reported only as total Th and its off-gas carryover rate was -1.1% and 12.5% before and after the PS sample adjustment, respectively. Although the positive carryover rate was a definite improvement, the post-adjustment carryover rate of 12.5% seems too high considering that ThO_2 has the highest melting point of all fuel oxides, including UO_2.[17] When the reported total Th was replaced with Th-232, whose SME concentration was also estimated based on its ratio to Fe in Tank 40 like the other radionuclides in Table 11 (except Cs-137), its carryover rate decreased to 3.8%, which still seems high compared to that of $\Sigma U_{isotope}$ but significantly lower than that of the reported total Th. It is noted that $\Sigma U_{isotope}$ and Th-232 made up >99% of the total mass of radionuclides in Table 11.

The off-gas carryover rate of Cs-137 also improved from the pre-PS adjustment value of <1%, which is too low based on its high relative volatility, to 14.2%, while that of Am-241, which constituted <0.02% of the measured PS sample radionuclides, increased from -4.6% to 9.5%. The marked improvements seen in the carryover rates of Th-232, Cs-137 and Am-241 further support; (1) the premise of the reported PS sample composition potentially being biased low in frit and (2) the approach taken to estimate the concentrations of the minor or even trace-level species using their ratios to Fe in Tank 40. On the other hand, the off-gas carryover rate of Tc-99 changed relatively little, from 82 to 84% and thus was insensitive to the PS sample adjustment. The >80% carryover rate is ~6X that of Cs-137 and higher than the SB7a projection of <60.2%.

5.2.4.3 Comparison of Overall Off-Gas Carryover Rates

The elemental off-gas carryover rates in Table 10 and Table 11 were calculated by comparing the MELT661 composition against the pre- and post-adjustment PS compositions. Three different overall carryover rates were calculated by; (1) summing up individual elemental carryover rates of the last MFT batch fed up to the point of PS sampling, e.g., MFT580 (Σelements) for SB7a, (2) subtracting the total mass of glass poured from the total calcine solids fed up to the point of PS sampling, e.g., MFT580 (Σoxides), and (3) subtracting the total mass of glass poured from the total calcine solids fed while processing all five MFT batches, e.g., MFT576-MFT580 (Σoxides). As noted earlier, the overall carryover rates of SB7b were calculated by including the entire MFT661 even though the PS sample was taken well before the MFT661 feeding was completed. The resulting SB7b carryover rates are compared to those of SB7a and SB6 in Table 12. Clearly, the overall elemental carryover rate of SB7b was the highest of the three at 2.8% of the calcine solids fed and decreased to 2.2% based on the overall mass balance of MFT661. The carryover rate was the lowest at 1.5% when the mass balance was extended over all five MFT batches. The overall elemental carryover rate of SB7b was somewhat higher than that of SB6 but lower than that of SB7a. No equivalent carryover rates of SB7a and SB6 were available to compare against the SB7b rates based on the overall mass balance.

Table 12. Comparison of Overall Off-Gas Carryover Rates.

Batch:	(% fed)
SB7b	
- MFT661 (Σelements)	2.8
- MFT661 (Σoxides)	2.2
- MFT657-MFT661 (Σoxides)	1.5
SB7a	
- MFT580 (Σelements)	3.7
- MFT580 (Σoxides)	-
- MFT576-MFT580 (Σoxides)	-
SB6	
- MFT551 (Σelements)	2.4
- MFT551 (Σoxides)	-
- MFT548-MFT551 (Σoxides)	-

6.0 Thermodynamic-Equilibrium Prediction of Off-Gas Carryover Rates

As a demonstration of the thermodynamic-equilibrium prediction of off-gas carryover rates, the SME660 composition in Table 13 was input into the FactSage software version 7.0 at the DWPF design basis glass production rate of 228 lb/hr,[18] and the resulting equilibrium flows of gas, melt (denoted as Slag-liq#1), and Invariant Condensed Phases (ICP) at 1,100 °C are given in Table 14. The SME660 composition was chosen because it was the last full batch fed to the melter prior to the PS sampling and thus would have been most representative of the melt composition. It is noted that most gas species in Table 13 except H_2O were added as a result of pre-decomposing the formate and nitrate salts not found in the FactSage database. For example, sodium formate and calcium nitrate were pre-decomposed as:

$$2\,NaCOOH = Na_2O + CO + CO_2 + H_2 \quad (17)$$

$$Ca(NO_3)_2 = CaO + N_2 + 2.5\,O_2 \quad (18)$$

Sodium diuranate was pre-decomposed as:

$$Na_2U_2O_7 = Na_2O + 2\,UO_3 \quad (19)$$

Table 13. Pre-Decomposed SME660 Input to FactSage Run.

Solids:	(lbmole/hr)		**Solids: (Cont'd)**	(lbmole/hr)
$Fe(OH)_3$	0.2186		NaF	0.0019
$Al(OH)_3$	0.2881		Na_2SO_4	0.0097
MnO_2	0.0276		Na_3PO_4	0.0033
MnO	0.0184			
CaO	0.0156		**Gases:**	(lbmole/hr)
UO_3	0.0170		CO	0.2320
$Mg(OH)_2$	0.0103		CO_2	0.2320
$Ni(OH)_2$	0.0424		H_2	0.2146
TiO_2	0.0037		N_2	0.0077
SiO_2	2.0507		O_2	0.0192
Na_2O	0.4022		H_2O	22.4645
B_2O_3	0.1735			
Li_2O	0.4086		**Properties:**	
Cs_2O (137)	5.33E-06		Total Solids	37.68%
TcO_2 (99)	5.06E-06		Calcine Solids	33.59%
ThO_2	0.0041		pH	6.00
$NaNO_3$	0.2244		PCCS WL	31.4%
NaCl	0.0050		Glass $Fe^{2+}/\Sigma Fe$	0.056

Each species in Table 14 is identified by its molecular formula followed by the name of the thermophysical database from which relevant property data was pulled. All gas species were assumed to form an ideal gas mixture based on the FactPS database, which contains pure substances data from standard compilations as well as the data for the compounds that have been evaluated/optimized to be thermodynamically consistent with the FACT solution databases such as FToxid.[18] All species in the Slag-liq#1 phase form a liquid solution optimized by the FToxid database, which contains the oxide system data for slags, glasses, minerals, ceramics, refractories, etc. Each species in the ICP forms a separate phase by itself.

Table 14. Equilibrium Partitioning of SME660 Using FactSage v7.0 at 1,100 °C and DWPF Design Basis Glass Rate of 228 lb/hr

PHASE: Gas	**lbmole/hr**		**PHASE: Slag-liq#1**	**lbmole/hr**
H_2O_FactPS	2.35E+01		Na_2O_FToxid	2.66E-01
CO_2_FactPS	4.64E-01		Al_2O_3_FToxid	2.57E-04
N_2_FactPS	1.20E-01		SiO_2_FToxid	1.45E+00
O_2_FactPS	9.75E-02		$NaAlO_2$_FToxid	2.88E-01
H_3BO_3_FactPS	1.16E-02		CaO_FToxid	5.10E-03
SO_2_FactPS	9.65E-03		FeO_FToxid	1.29E-02
HBO_2_FactPS	7.40E-03		Fe_2O_3_FToxid	3.03E-02
$LiBO_2$_FactPS	3.54E-03		NiO_FToxid	4.24E-02
$NaBO_2$_FactPS	2.61E-03		MnO_FToxid	3.96E-02
HCl_FactPS	2.37E-03		B_2O_3_FToxid	4.02E-02
HF_FactPS	1.88E-03		$NaBO_2$_FToxid	2.41E-01
NaCl_FactPS	1.76E-03		Mn_2O_3_FToxid	3.20E-03
LiCl_FactPS	8.66E-04		P_2O_5_FToxid	2.54E-04
OH_FactPS	6.75E-04		TOTAL_2 :	2.42E+00
LiOH_FactPS	6.69E-04			
NaOH_FactPS	2.12E-04		**PHASE: Invariant Condensed**	**lbmole/hr**
NO_FactPS	1.80E-04		$Li_2Si_2O_5$_Solid_II(s2)_FactPS	2.01E-01
H_2_FactPS	1.09E-04		Li_2SiO_3_solid(s)_FactPS	2.01E-01
SO_3_FactPS	4.69E-05		Fe_2O_3_hematite(s)_FToxid	7.25E-02
$Ni(OH)_2$_FactPS	3.37E-05		$(CaO)(UO_3)$_solid(s2)_FactPS	1.05E-02
LiF_FactPS	1.50E-05		ThO_2_Thorianite(s)_FactPS	4.10E-03
$(HBO_2)_3$_FactPS	1.33E-05		Li_3PO_4_solid(s)_FToxid	2.79E-03
$CsBO_2$_FactPS	8.73E-06		U_3O_8_solid(s)_FactPS	2.17E-03
Na_2SO_4_FactPS	4.46E-06		TOTAL_3 :	4.94E-01
CO_FactPS	4.36E-06			
$Fe(OH)_2$_FactPS	3.99E-06		**REDOX:**	
NaF_FactPS	3.77E-06		- $Fe^{2+}/\Sigma Fe$	0.059
Cl_FactPS	3.07E-06			
Tc_2O_7_FactPS	2.53E-06		**Calculated Volatility (% fed):**	
UO_3_FactPS	2.50E-06		- Cs	100.0%
OBF_FactPS	1.93E-06		- Tc	100.0%
CsCl_FactPS	1.66E-06		- Th	0.0%
$UO_3(H_2O)$_FactPS	1.40E-06		- U	0.0%
$(NaCl)_2$_FactPS	1.31E-06		- S	~100.0%
Li_2SO_4_FactPS	6.21E-07		- Cl, F	~100.0%
$(LiCl)_2$_FactPS	3.06E-07		- B	7.3%
CsOH_FactPS	2.64E-07		- Na	0.4%
TOTAL_1 :	2.42E+01		- Li	0.6%

Table 14 shows that 100% of Cs and Tc would volatilize as $CsBO_2$/CsCl and Tc_2O_7, respectively, under the thermodynamic equilibrium conditions at 1,100 °C and these predicted volatilities are significantly higher than their respective off-gas carryover rates of 14.2% and 84.3% in Table 11. This was expected as the thermodynamic-equilibrium predictions are solely based on the vapor pressures of specific compounds that are favored to form in the absence of any mass transfer resistances such as; (1) the cold cap which acts as a physical barrier to the volatiles emission, (2) bulk diffusion of volatile species through the melt pool to the melt surface or the bubble-melt interface, and (3) loss of both volatiles and non-volatiles due to off-gas surging induced by the cold cap instabilities (i.e., physical entrainment). Likewise, nearly 100% of S and halides (Cl and F) were also predicted to volatilize, although the results of the FactSage run in Table 14 are only preliminary because the other FACT databases such as FTsalt or other FToxid database options were not fully explored. The predicted volatilities of U and Th were essentially zero, which suggests that the low but non-zero carryover rates of $\Sigma U_{isotope}$ and Th-232 in Table 10 were likely due to the physical entrainment rather than their relative volatilities. The most volatile frit component was boron at 7.3% volatility, as it formed borates of Na, Li and Cs. This is consistent with the observed loss of ~2.5% boron fed as H_3BO_3 during the frit fabrication at 1,100 °C in a crucible with a loose-fitting lid.[19]

The calculated REDOX of the SME660 glass ($Fe^{2+}/\Sigma Fe$) was essentially identical to the PCCS value, 0.059 vs. 0.056, which gives credence to the calculated equilibrium speciation using the FactSage code. This has a large implication on the predicted volatility of those species that exhibits a strong dependence on REDOX such as Tc. For example, the calculated off-gas carryover rate of 84.3% for Tc-99 at the measured PS glass REDOX of 0.07, thus practically as oxidizing as the SME660 glass, suggests that the high carryover rate of Tc-99 in the form of highly-volatile Tc_2O_7 was plausible and further aided by the fact that the melter feeding was interrupted frequently while feeding MFT661, which would have exposed a significant area of melt surface for the volatiles emission.

7.0 Discussion

The calculated off-gas carryover rates of SB7b using the adjusted PS glass composition are compared with those of SB6/SB7a and the measured data during the DM1200 melter run at VSL in Table 15 and further discussed in terms of melter operating variables and feed/glass chemistry. Off-gas carryover is strongly scale-dependent, i.e., the larger the melt surface area, the greater the potential for carryover. The DM1200 was chosen as it was the largest VSL melter used for relevant off-gas emission tests and is at just under ½ scale of the DWPF melter based on melt surface area.

7.1 Impact of Bubbling on Off-Gas Carryover

During the DM1200 run,[8] the HLW AZ-101 simulant was fed along with the glass-forming chemicals (in lieu of frit) under different bubbler configurations and using air as the bubbling gas (vs. argon for the DWPF melter). A clear trend is seen in the DM1200 data in Table 15 that both the elemental and overall off-gas carryover rates increased (except F) and nearly doubled for most waste components when the bubbling flux, defined as bubbling rate per unit melt surface area, was doubled from Test 9A to 9B. For the glass-former components such as B and Si, the increase was not quite 2X but still >50%. This trend was expected based on the data from the same DM1200 test; when the number of bubblers was doubled to four at the same total bubbling rate, thereby reducing the linear bubbling velocity by 50%, the measured off-gas carryover rates of all species decreased as a result, which suggests that physical entrainment would increase with increasing linear bubbling velocity. Furthermore, under bubbled conditions, the DWPF melter pressure spikes were shown to be significantly larger and more frequent than under non-bubbled conditions,[20] and it is during those large melter pressure spikes that significant quantities of the feed and glassy materials can become airborne and entrained in the melter exhaust, i.e., physical entrainment. This is supported by the measured chemical composition of the off-gas deposit samples, which indicates that the off-gas deposits were likely a combination of sludge and frit particles entrained in the off-gas.[6]

Table 15. Comparison of DWPF vs. DM1200 Melter Off-Gas Entrainment Ratios.

Melter	DWPF			DM1200	
Melt Surface Area (ft^2)	28.3			12.9	
Feed	SB6	SB7a	SB7b	AZ-101 simulant	
Bubbling Flux ($scfm/ft^2$)	0.18	0.20	0.15	0.18	0.36
# of Bubblers	4[1]			2[2]	
Bubbling Medium	Argon			Air	
Reductant	Formic Acid			Sugar	
Glass REDOX ($Fe^{2+}/\Sigma Fe$)	0.38	0.13	0.07	0.06 - 0.10	
Off-Gas Carryover	(% Fed)	(% Fed)	(% Fed)	(% Fed)	(% Fed)
Al	3.3	<8.8	2.3	0.44	0.81
B	1.9	1.0	1.3	2.03[3]	3.18[3]
Ba	-27.6	2.1	2.7	0.64	1.38
Ca	-9.5	-4.0	-8.8	1.08	1.59
Cd	18.2	3.8	0.8	2.32	2.68
Cr	-360	-38.7	-74.8	-	-
Cs-137	16.4	13.6	14.2	-	-
Cu	-628	-754	-416	0.60	1.04
F	-	-	-	81.58[3,4]	36.99[3]
Fe	0.7	2.2	6.8	0.93	1.91
K	46.2	-	-	5.21	5.68
Li	0.9	0.8	2.5	0.44	0.75
Mg	0.2	-2.6	7.1	1.88	3.23
Mn	5.6	0.1	6.8	0.32	0.66
Na	7.5	<14.2	5.1	1.02	1.88
Ni	-5.6	-0.9	12.2	0.58	1.08
Pb	-36.9	-	-44.0	1.10	2.00
Ru	-25.4	27.8	55.5	4.08	6.18
S	> 49.2	-	8.0	67.47[3]	70.96[3]
Si	0.6	0.6	2.1	0.35	0.52
Sr	-8.1	-2.5	7.1	1.03	2.29
Tc-99	-	<60.2	84.3	-	-
Th-232	13.6	4.5	3.8	-	-
Am-241	5.4	7.7	9.5	-	-
$\Sigma U_{isotope}$	5.4	-5.3	1.3	-	-
Zn	-160	-269	-125	0.93	1.62
Zr	31.2	-2.1	45.7	0.36	0.64
Overall (Σelements)	2.4	3.7	2.8	-	-
Overall (mass balance)	-	-	1.5[6]	0.62[5]	1.11[5]

[1] Each with one outlet; [2] Each with two outlets; [3] Includes particulate & gas samples; [4]From water dissolution of filter particulate; [5] From gravimetric analysis of filters and rinses; [6] From mass balance: total calcine solids fed – total glass poured over 5 MFT batches.

The impact of bubbling on off-gas carryover rate is not as clearly manifested by the DWPF data most likely because of the relatively narrow range of bubbling fluxes used. When the bubbling flux was decreased from 0.18 scfm/ft^2 (SB6) to 0.15 scfm/ft^2 (SB7b), the calculated carryover rates of Al, B, Na, Cs-137, Th-232 and $\Sigma U_{isotope}$ decreased, as expected, while others such as Fe and Si showed the opposite trend. Regardless, the overall off-gas carryover rates of SB7b and DM1200 melter were 1.5% and 1.1%, respectively. As expected, these carryover rates were higher than the DWPF design basis of 1% for non-bubbled operation.[15]

7.2 Impact of REDOX on Tc Volatility

The oxidation state of a multivalent element in glass and its resulting volatility depend on the concentration of dissolved O_2, as manifested by the measured iron REDOX ratio, $Fe^{2+}/\Sigma Fe$. Of particular interest is the volatility of Tc-99 which is known to increase with increasing oxidation state.[21] In Table 11, the off-gas carryover rate of Tc-99 was estimated at 84.3% at the measured SB7b glass REDOX of 0.07, which is found to be in close agreement with the measured Tc-99m retention of 18% in a glass prepared without any reductants or 82% volatility, when Tc was fed as ammonium pertechnetate (NH_4TcO_4).[22] Furthermore, the FactSage model predicted 100% volatility of Tc from the SME660 glass as Tc_2O_7; however, a recent study concluded that Tc would likely volatilize as alkali pertechnetates, predominantly as $KTcO_4$, rather than decomposing into alkali oxides and extremely-volatile Tc_2O_7.[23] Notwithstanding the fact that the alkali pertechnetates are missing from the FactSage database, the discrepancy in the likely form of volatile Tc in the melter should not impact the quantitative results on the carryover since Tc_2O_7 and pertechnetates have the same +7 oxidation state and thus both evidently have high volatilities under oxidizing conditions.

In fact, as the alkali pertechnetates have melting points ranging from 378 to 595 °C,[24] it is conceivable that some of the lower melting-point pertechnetates would decompose into Tc_2O_7 and oxides (e.g., $2NaTcO_4 \rightarrow Tc_2O_7 + Na_2O$) and the latter combine with B_2O_3, whose melting point falls in the lower range of alkali pertechnetates, to form semi-volatile borates (e.g., $Na_2O + B_2O_3 \rightarrow 2NaBO_2$), as predicted by the FactSage model in Table 14. The presence of alkali borates was also confirmed in the DWPF melter off-gas deposit samples.[25] When the REDOX was increased to 0.13 in the SB7a glass, the estimated carryover rate of Tc-99 decreased to <60.2%, which is consistent with the inverse relationship between Tc volatility and glass REDOX. At the measured REDOX of 0.38, the SB6 glass was considerably more reducing than either the SB7a or SB7b glass and the Tc volatility would have been lower; however, the decreasing trend could not be confirmed as the concentration of Tc-99 in Tank 40 and the PS sample was both below detection limit.

7.3 Impact of Temperature on Off-Gas Carryover

As the temperature of the DWPF melt pool is controlled nominally at 1,150 °C, its impact on the off-gas carryover is not discernable from the DWPF data. However, it is expected that any volatile species would become less volatile as the temperature decreases and two studies attempted to measure the volatility of Tc at varying temperatures. In the first study,[24] the feed containing NH_4TcO_4 was heated in a platinum crucible from room temperature to the final temperature ranging from 900 °C to 1,350 °C. Once the final temperature was reached, the sample was either quenched immediately or allowed to "dwell" at that temperature for 30 minutes before quenching. As expected, the measured volatility was the lowest at 900 °C with zero dwell time but was still quite high at ~80%. The highest volatility was 99.3% at 1,350 °C with 30-min dwell time but it dropped to ~90% with zero dwell time, which shows the effect of mass transfer resistance even in the small melt volume in a crucible. No REDOX data was given but measured volatilities were high regardless of the glass temperature or dwell time.

In the second study,[22] the DM10 melter at the VSL, whose melt surface is only 1/125th of the DWPF melter, was fed with a simulated Hanford tank waste spiked with Tc-99m in the form of NH_4TcO_4 at 1,050 to 1,200 °C. The Tc-99m retention in the baseline glass reached 76% at 1,050 °C, which would mean 24% volatility based on the mass balance. Although the reported volatility was lower at 18%, it increased to 32% at 1,150 °C, thus confirming at least the qualitative trend of increasing volatility with increasing glass temperature.

7.4 Additional Factors Affecting Off-Gas Carryover

Although all three DWPF feeds were blended with the same Frit 418 and fed under similar bubbling fluxes, the calculated elemental carryover rates were quite different, which suggests that the feed chemistry played a key role. The feed chemistry is determined not only by the compositions of the waste and the frit (or glass-forming chemicals) but by the ratio of the two or WL. For example, when the DWPF sludge simulant was blended with a high-alkali frit, thus lowering the melt viscosity, the measured carryover rates under non-bubbled conditions were found to be comparable to those under bubbled conditions when the same simulant was blended with a low-alkali frit.[9] It is postulated that less viscous melts are more prone to cause the cold cap instability, which in turn increases the likelihood of off-gas surging and thus physical entrainment of the feed/glassy materials into the off-gas system. The loss due to physical entrainment can only be discerned from the data taken from continuously-fed prototypic melters, not from bench-scale melter or crucible tests.

Furthermore, it was shown earlier that as the WL increased, the feed became more difficult to melt,[26] and the X-ray computed tomography (CT) analysis of the partially-melted batch showed that the decrease in melting rate was due to the excess amount of gas generated from the decomposing salts, e.g., nitrate, which increases the tendency for foaming and off-gas surging.[27] Thus, it is expected that off-gas carryover will increase with increasing WL. The calculated off-gas carryover rates of the DWPF feeds are compared in terms of WL in Table 16 and the expected trend between carryover and WL is seen between SB6 and SB7a but not SB7b. However, the 2.8% carryover rate of SB7b could be an anomaly as the MFT661 attainment was particularly low at 63.3% compared to SB6 and SB7a due to frequent feed interruptions. The premise is that the feed tube flushing done after each feed pump stop and before each feed pump restart produces melter pressure spikes, which increases the potential for physical entrainment in addition to the loss of volatiles during the idling periods. This premise is supported by the fact that the overall carryover rate of SB7b fell to 1.5%, as shown in Table 12, which was calculated from the overall mass balance as: (total calcine solids fed – total glass poured while processing MFT657-MFT661) / total calcine solids fed. Clearly, additional sludge batch cases need to be looked into in order to produce more data from which to drive a correlation between the carryover rate and feed chemistry, specifically in terms of REDOX, viscosity, WL, alkali content, etc. Interestingly, when the calculated WL of 36.8% for the PS sample is used in lieu of that of SME660 in Table 16, the calculated carryover rates of SB6, SB7a and SB7b correlate with WL.

Table 16. Off-Gas Carryover vs. DWPF Glass WL.

Run	SB6	SB7a	SB7b
Batch	MFT551	MFT580	MFT661
PCCS WL*	34.5	37.9	31.4
Batch Attainment	~100%	93.9%	63.3%
Carryover (Σ elements)	2.4	3.7	2.8

* For the SME550, SME579 and SME660, respectively.

7.5 Additional Thoughts on Elemental Carryover Rates

As shown in Table 7, Si was by far the most abundant (by weight) of all elements in every SB7b MFT batch followed by Na, Fe, Al, Li, U and B in the order of decreasing abundance. When they were partitioned into the sludge and frit groups, the sum of the major sludge components at concentration > 1 wt% in the MFT661 was 61% of the sum of all frit components or the sludge/frit mass ratio of 0.61. The corresponding ratio in the off-gas carryover was calculated to be higher at 1.31, which means that the relative carryover tendency of the sludge group was ~2X that of the frit group. By comparison, the sludge/frit ratio in the quencher deposit sample taken in 2007 was calculated to be much higher at 4.9 using the average analytical data, which was copied from Table 1 of Reference 6 into Table 17. The same ratio of the "matching" feed could not be determined as the quencher deposit had been accumulating over time and thus its chemistry (i.e.,

analytical results) reflected previous MFT batch compositions processed prior to the time when the deposit samples were taken. Nevertheless, the sludge/frit mass ratio of the feed cannot be much greater than that of MFT661, 0.61, unless the WL approaches near 50%. To confirm this, the reported analytical results of the SME388, which was processed in December 2006 as part of SB3, was added to the last column of Table 17 and the sludge/frit mass ratio was calculated to be a little higher at 0.68. Thus, the relative carryover tendency of the SB3 sludge was ~7X that of the frit (i.e., 4.9/0.68 = 7.2), which means that the sludge group was more prone to carryover than the frit group during SB3 than SB7b or, equivalently, the frit group was less prone to carryover during SB3 than SB7b. Since the main difference in the DWPF melter operation between 2007 and 2013 was the use of glass bubblers during SB7b but not during SB3, the results appear to suggest that the frit particles become comparatively more prone to carryover than the sludge counterparts when the glass bubblers are in use.

Table 17. Analytical Results of DWPF Quencher Deposit Sample (Data Taken from Ref. 6).

Element	Quencher-1	Quencher-2	Quencher-3	Average	SB3	SME388
	(wt% CS)	(wt% CS)	(wt% CS)	(wt% CS)	(wt% CS)	(wt% CS)
Ag	0.018	0.017	0.016	0.017	0.016	
Al	4.61	4.57	4.53	4.57	5.14	2.69
B	0.3	0.32	0.31	0.31	0.015	1.47
Ba	0.04	0.04	0.042	0.041	0.048	
Ca	1.12	1.53	1.49	1.38	1.61	0.70
Cd	0.39	0.49	0.42	0.43	0.18	
Cr	0.077	0.074	0.068	0.073	0.11	0.06
Cu	0.016	0.014	0.015	0.015	0.027	0.01
Fe	10.6	9.92	10.5	10.3	16.4	7.66
Hg	0.15	0.15	0.12	0.14	0.15	
Li	0.17	0.18	0.18	0.18	0.039	2.16
Mg	1.08	1.21	1.11	1.13	1.52	0.68
Mn	2.45	2.35	2.4	2.4	3.56	1.49
Na	4.73	4.88	4.57	4.73	13.1	9.14
Ni	0.63	0.59	0.62	0.61	0.98	0.47
P	0.23	0.2	0.26	0.23	0.44	
S	1.65	1.88	1.98	1.84	0.38	0.02
Si	4.4	3.54		3.97	1.06	25.07
Sr	0.2	0.28	0.27	0.25	0.37	
Ti	0.01	0.01	0.01	0.01	0.016	0.07
U	5.68	5.47	5.06	5.4	6.77	2.48
Total	38.551	37.715	33.971	38.026	51.9	54.2
Sludge =				30.08		21.63
Frit =				6.13		31.94
Sludge/Frit =				4.90		0.68
Fe/Al =				2.25		2.85

Although B and Li are two of the main feed components and considered to be more volatile than Fe, Al or Si, their concentrations in the off-gas deposits were relatively low. For example, a loss of 2.5% B was observed during the frit fabrication process at 1,100 °C for 30 min,[19] and the volatility of Li was predicted by the FactSage model and confirmed by its presence in the off-gas deposit samples as alkali borate salts.[24] Nevertheless, the B/Si and Li/Si ratios in the off-gas deposit samples were an order-of-magnitude lower than their respective ratios in Frit 418.[6] Furthermore, as all of the identified species in the quencher deposit sample except for S and, to a lesser extent, Na are considered to be nonvolatile, both SB3 (measured) and SB7b (calculated) off-gas carryover results strongly suggest that under actual production melter settings, physical entrainment may account for the bulk of off-gas carryover. From a melter operational standpoint, the key to limiting the carryover of volatiles would be to maintain as high a cold cap coverage as practically possible without flooding the melter, since the tendency for the cold cap instability and thus off-gas surging increases with increasing cold cap coverage, which is directly related to the nonvolatiles carryover.

It is also noted that the calculated carryover rates of Cs-137 remained relatively steady from 13.6% (SB7a) to 16.4% (SB6) with that of SB7b at 14.2%, regardless of varying bubbling flux, REDOX and WL. The calculated carryover rates of Th-232 and Am-241 were similar at 4-10%, while that of Sr-90 remained high between 21.5% (SB7b) and 34.6% (SB7a). The calculated carryover rate of Np-237 was 5.7% for SB7b but were negative for SB6 and SB7a. One common thread for these radionuclides is that except for Th-232, their Tank 40 concentrations were <0.01 wt% on a total solids basis and their SME concentrations except for Cs-37 were estimated using their respective ratios to Fe in Tank 40. Thus, there is a need for checking the adequacy of calculated carryover rates of these minor or trace-level species based on the estimated feed concentrations against data. However, the analytical data on the off-gas deposits alone will not be enough to close the mass balance because the analyzed deposits had been accumulating over time and it is unlikely that not only the feed composition but the melter operating conditions remained unchanged during that time.

After accounting for the nonradioactive fraction of cesium in the waste, which is estimated to be ~77%,[28] the calculated carryover rates of cesium and Tc-99 were 4.5E-6 and 2.1E-6 lbmole/hr, respectively, based on the DWPF design basis glass production rate of 228 lb/hr. Thus, on a molar basis, the loss of cesium to the off-gas was more than 2X that of Tc-99. By comparison, the calculated carryover rates of cesium and Tc-99 during SB7a were 5.0E-6 and 3.2E-6 lbmole/hr, respectively, or the cesium to Tc-99 molar carryover ratio of 1.6. These results show that there was more than enough cesium to volatilize 100% Tc as $CsTcO_4$, if indeed $CsTcO_4$ is the most volatile and TcO_2 the least volatile as in pure phases.[21] It is unclear how this would be influenced by the complex matrix of the DWPF glass or its REDOX. Furthermore, it is not known what the chemical form of Tc is in the DWPF feed, as it could be pertechnetate ion in interstitial water or trapped in sludge particles or could be TcO_2. Further experimental work would be needed to determine the actual volatile species and contributors to its volatility.

The negative entrainment rates (shown in red text in Table 15) indicate that more material was measured in the PS sample than was predicted by the mass balance. In some cases, the method of matching the ratios to Fe in Tank 40 to estimate the corresponding concentrations in the SME did not yield meaningful results particularly for the minor or trace-level constituents because of their high sensitivity to the variations in the input data. In other cases, the glass sample appeared to contain metals leached out of the melter refractory or contamination during laboratory procedures. For example, Cu and Zn consistently have large negative carryover rates ranging from -416% to -628% and from -125% to -269%, respectively, in all PS samples analyzed thus far due to the combination of being present in the MFT at <0.05 wt% (on a calcine basis) and their concentrations in the PS sample increasing nearly by an order of magnitude. In preparation for the analysis, the glass was ground using agate grinding tools and sieved.[13] The sieves were most likely made of brass wire, and some of the brass could potentially be abraded onto the glass particles and appear as Cu and Zn in the final analysis, artificially appearing as negative entrainment rates.

The calculated carryover rate of Ca remained relatively steady for all three feeds but negative ranging from -4% to -9.5%, while that of Cr also remained negative but varying more widely from -39% (SB7a) to -75% (SB7b) – note that the rate of -360% for SB6 was considered an outlier. The leaching of melter components may explain the negative aspect of Cr carryover rates. First, its concentration in the MFT was lower than either Al or Fe by more than two orders of magnitude so even a slight change in the SME or PS sample analytical data or the metal leaching/corrosion rates would have a very large impact on its carryover rate. Second, chromium is a major constituent of both K-3 refractory (27 wt% as Cr_2O_3) and Inconel 690™ electrodes (27-31 wt%). Thus, considering the age of the DWPF melter running at that time (i.e., Melter #2 had been in operation for over 10 years vs. its design life of 2 years), a small quantity of Cr could have entered the glass pool from the leaching of either K-3 or Inconel 690™, more likely from the latter unless chromium could selectively leach out of K-3.

On the other hand, nickel showed negative carryover rates for SB6 and Sb7a but not for SB7b. However, since its concentration in the feed was ~40X higher than that of Cr, its calculated entrainment ratio should have been less sensitive to the variations in analytical data or leaching/corrosion rates. Thus, the fact that ~60 wt% of Inconel 690™ is made up of Ni suggests that the negative entrainment rate of Ni for SB6 and SB7a may have been due to leaching of Inconel 690™. This scenario is likely if the electrodes are in or near the path of rising argon bubbles, as demonstrated in a recent melter study using a K-3 coupon inserted into the melt pool directly in the path of bubbles.[29] The fact that the calculated entrainment rate of Ni was negative for SB6 and continued to be negative for SB7a adds credence to the postulation of leaching of Inconel 690™ electrodes. Furthermore, the fact that the bubblers also made of Inconel 690™ need to be replaced regularly due to significant corrosion near the cold cap, where the rising bubbles turn horizontal presumably hitting the bubblers directly, is another source for Ni and Cr outside the feed. Although the positive carryover rate of Ni for SB7b may be qualitatively explained in term of the lower bubbling flux used but the relatively small decrease in bubbling flux does not seem enough to explain a sudden reversal of carryover direction. This needs to be examined further when the calculations are repeated in a future study using the data taken during non-bubbled melter operation. It would also be interesting to see how the calculated carryover rates of Cr, Ni or even Al would change as the method is applied to the current sludge batch (SB9) being fed to the new Melter #3.

Two most dominant sludge components besides Na are Al and Fe, and their relative carryover behaviors during SB7b are compared in terms of Fe/Al ratios in the feed vs. in the off-gas carryover. It turns out that the Fe/Al ratio in the projected off-gas carryover was ~3X that in the feed, which would mean that iron had a ~3X higher carryover tendency than aluminum. By contrast, the Fe/Al ratios in the SME388 and the 2007 quencher deposit sample were more comparable, i.e., 2.85 vs. 2.25, which would mean that the relative carryover tendency of Fe was ~80% that of Al during SB3. It is also noted that despite their known volatility, the calculated carryover rates of Cd and S were only 0.8% and 8.0%, respectively, while their respective SB6 rates were more in the expected range of 18.2% and >49.2%, respectively. Since the concentration of S in the SB7b was ~4X that of SB6 and above the conservative PCCS limit for sulfur solubility in glass, the excess concentration of S in SB7b could have increased its carryover rate. Additional sludge batch cases need to be studied to filter out any outliers in the results.

7.6 Comparison with DM1200 Data

A direct comparison between the DWPF and DM1200 melter carryover rates is not straightforward and thus is not guaranteed to produce meaningful conclusions because off-gas carryover is impacted by a host of variables including the feed chemistry, bubbling flux, and melter design and operating characteristics. For example, when the SB6 simulants treated with three different reductants, including formic acid, glycolic acid and sugar, were fed to the DM10 melter at VSL, the resulting off-gas from the formic acid-treated feed was found to fluctuate more frequently with greater amplitude than the other feeds.[30] Fluctuating off-gas flow is an indication of off-gas surging, which provides the driving force for the entrainment of nonvolatiles.

If the calculated carryover rates from the DWPF melter are compared with those from the DM1200 at the same bubbling flux of 0.18 scfm/ft^2 solely based on the reductants used, the former with the formic-acid treated feed were indeed higher than the latter with the sugar-treated feed, which is qualitatively in line with the large variances in measured off-gas concentrations during the DM10 run. Focusing only on the major feed constituents, the calculated DWPF carryover rates are higher than their DM1200 counterparts by up to 7X (for Fe). However, it does not seem plausible that use of formic acid was the main reason for such a large increase in off-gas carryover. Two main exceptions are B and S. The higher carryover rate of B from the DM1200 is likely because boron was added as boric acid instead of more refractory B_2O_3, as in the DWPF. Conversely, the volatility of S is more complex to predict as it depends heavily on feed chemistry, which in turn affects the solubility limit of S in glass, formation of sulfides, etc. It is likely that the calculated low volatility of S in SB7b is an outlier; otherwise, the DWPF and DM1200 carryover rates in Table 15 are in closer agreement.

On the other hand, the much higher DWPF carryover rates of Na and semi-volatiles such as Cd (if indeed the SB7b rate was an outlier) and Cs than their DM1200 counterparts could be reflective of actual melter conditions leading up to the PS sampling such as extended idling and/or perhaps more frequent off-gas surges of larger-magnitudes. In the future study, the calculated carryover rates of individual species will need to be interpreted by tracking the melter operating history more closely.

8.0 Conclusions

The results of this work demonstrate the feasibility of estimating the off-gas carryover rates from the DWPF melter based on the overall as well as elemental mass balances using the measured SME product and glass pour stream compositions and time-averaged melter operating variables over the duration of one canister filling cycle. The first two case studies performed earlier involved the SB6 and SB7a PS glass sample.[4-5] In this work, a third case study was performed involving the SB7b PS glass sample collected on 3/18/2013 at 10:28 hour while Canister #4023 was being filled under bubbled conditions. Based on the results presented and subsequent discussions given in this report, it is concluded that:

1. The proposed method of estimating off-gas carryover (or entrainment) rates from measured feed and pour stream glass compositions appears feasible and thus additional case studies are warranted. However, success of this approach requires that the analytical data for the feed and pour stream glass be both accurate and consistent and all relevant melter operating data be interpreted, analyzed, and applied correctly.

2. The overall SB7b entrainment rate from the bubbled DWPF melter was calculated to be 1.5% of the calcine solids fed based on the mass balance between the total calcine solids fed and the total glass poured over five MFT batches. This rate is 50% higher than the design basis entrainment rate for the non-bubbled melter but is in line with recent results of SB6 and SB7a.

3. The sum of the elemental carryover rates of five major nonvolatile sludge components, i.e., Al, Fe, Mn, Ni, and U, was 5.2%, while that of the frit components, including Si, B, Li but not Na, was 2.1%. The calculated carryover rate of 5.2% for the sludge group is skewed high because that of Fe was high at 6.8%; Fe accounted for 43% of the major sludge components at concentration >1%.

4. The sludge/frit mass ratio in the off-gas carryover was 2X that in the MFT661, which indicates that the relative carryover tendency of the sludge as a group was 2X that of the frit. By comparison, the sludge/frit mass ratio in the quencher deposit sample taken in 2007 was 7X that in the SME388 that was fed in December 2006 as part of SB3, which is consistent with the SB7b results; the sludge was more prone to carryover than the frit. Since the main difference in the DWPF melter operation between 2007 and 2013 was the use of glass bubblers during SB7b but not during SB3, the much lower sludge/frit mass ratio in the SB7b carryover suggests that the frit particles are comparatively more prone to carryover than the sludge counterparts when the glass bubblers are in use.

5. When the measured glass REDOX (i.e., $Fe^{2+}/\Sigma Fe$) was decreased from 0.13 (SB7a) to 0.07 (SB7b), the calculated carryover rate of Tc-99 increased from <60.2% to 84.3%, as would be expected under more oxidizing conditions.

6. The calculated carryover rate of Cs-137 was 14.2%, which means that the carryover rate of Cs-137 remained relatively steady between 13.6% (SB7a) and 16.4% (SB6) regardless of the bubbling flux, REDOX and WL tested.

7. The calculated carryover rate of sulfur was unexpectedly low at 8%, compared to >49% for SB6. It is suspected that the low SB7b carryover rate of S also may have been affected by the seemingly-biased PS glass composition.

8. The impact of bubbling flux on the carryover rate was not conclusive. When the bubbling flux was decreased from 0.18 scfm/ft^2 (SB6) to 0.15 scfm/ft^2 (SB7b), the calculated carryover rates of Al, B, Na, Cs-137, Th-232 and $\Sigma U_{isotope}$ all decreased, as expected. However, Fe and Si showed the opposite trend. Tc was below detection limit in the SB6 glass so could not be compared.

9. The FactSage code was run using the SME Batch 660 (SME660) composition and the results showed that:

    9-1. 100% of Cs and Tc would volatilize as $CsBO_2$/CsCl and Tc_2O_7, respectively, under the thermodynamic equilibrium conditions at 1,100 °C. These predicted rates represent the thermodynamic maximum in the absence of any mass transfer resistances such as the presence of the cold cap and bulk diffusion through the glass melt.

    9-2. The predicted volatilities of U and Th were essentially zero, which means that the low but non-zero carryover rates of U and Th-232 calculated based on the SB7b data were likely due to physical entrainment rather than their relative volatilities.

    9-3. 7.3% of boron fed was predicted to volatilize as alkali borates vs. the calculated volatility of 1.3% based on SB7b data.

    9-4. The predicted REDOX of SME660 glass was 0.059 vs. the measured value of 0.056, i.e., they are essentially identical.

10. The calculated DWPF melter carryover rates of the major feed components were higher than their DM1200 counterparts by up to 7X (for Fe). Two main exceptions are B and S. The higher carryover rate of B from DM1200 is likely because boron was added as boric acid instead of more refractory B_2O_3, as in the DWPF feed.

9.0 Future Work

The proposed mass balance approach will be tested further using additional pour stream glass data taken under different conditions (e.g., non-bubbled operation and varying feed compositions) and, if necessary, will be adjusted and refined. In particular, work needs to focus on; (1) quantifying the uncertainty bounds of both analytical and key melter operating data, and (2) better estimation of melter hold-up of various elements and process delays due to the cold cap reactions. Data permitting, work also needs to be expanded by including other isotopes besides Cs-137 and Tc-99. Future work also includes completing the remaining tasks necessary to enable incorporation of the off-gas carryover correlations into the WTP flowsheet models. As stated in the Introduction, these tasks include; (1) completion of the collection and evaluation of all available DWPF sludge batch data, (2) thermodynamic modeling of the vitrification process, and (3) aqueous electrolyte modeling of the melter off-gas condensate chemistry.

10.0 Quality Assurance

The work defined herein is not waste form affecting, and thus does not need to follow QA requirements of RW-0333P. This technical report does not support any Type 1 calculation and thus need not be treated as a lifetime record. Data entry and calculations were performed by A. S. Choi following the steps used in the previous studies.[4-5] D. L. McClane performed a technical review of calculations following the requirements for performing reviews of technical reports and the extent of review, as defined in Manual E7, Procedure 2.60, including the input/output.

11.0 References

1. EMSP Project Test Plan, "Technetium Management – Hanford Site (FY2015)," ***TP-EMSP-0018***, ***Rev. 0***, U.S. Department of Energy, April 2015.

2. Ray, J. W., Culbertson, B. H., Marra, S. L., and Plodinec, M. J., "DWPF Glass Product Control Program," ***WSRC-IM-91-116-6***, ***Rev. 7***, Washington Savannah River Co., Aiken, SC, 2012.

3. DWPF Waste Form Compliance Plan (U), ***WSRC-IM-91-116-0***, ***Rev. 12***, Savannah River Remediation, Aiken, SC, September 2018.

4. Choi, A. S., Kesterson, M. R., Johnson, F. C., and McCabe, D. M., "Preliminary Analysis of Species Partitioning in the DWPF Melter," ***SRNL-STI-2015-00279, Rev. 0***, Savannah River National Laboratory, Aiken, SC, July 2015.

5. Choi, A. S., Smith, F. G., and McCabe, D. M., "Preliminary Analysis of Species Partitioning in the DWPF Melter – Sludge Batch 7a," ***SRNL-STI-2016-00540, Rev. 0***, Savannah River National Laboratory, Aiken, SC, January 2017.

6. Zeigler, K. E., and Bibler, N. E., "Characterization of DWPF Melter Off-gas Quencher and Steam Atomized Scrubber Deposit Samples," ***WSRC-STI-2007-00262***, ***Rev. 0***, Savannah River National Laboratory, Aiken, SC, May 2007.

7. McCabe, D. J., and Choi, A. S., "Task Technical and Quality Assurance Plan for Technetium Management – Flowsheet Modeling Improvements for LAW Recycle Predictions," ***SRNL-RP-2014-01062, Rev. 0***, Savannah River National Laboratory, Aiken, SC, October 2014.

8. Matlack, K. S., Weiliang, G., Bardakci, T., D'Angelo, N., Lutze, W., Callow, R. A., Brandys, M., Kot, W. K., and Pegg, I. S., "Integrated DM1200 Melter Testing of Bubbler Configurations Using HLW AZ-101 Simulants," ***VSL-04R4800-4***, ***Rev. 0***, Catholic University of America, Washington D.C., August 16, 2004.

9. Sabatino, D. M., "Sampling Data Summary for the Ninth Run of the Large Slurry Fed-Melter," ***DPST-83-1032***, Savannah River Laboratory, Aiken SC, November 22, 1983.

10. Hodges, B. C., *Unpublished DWPF Melter Operating Data (SB7b)*, Savannah River Remediation, Aiken, SC, April 2018.

11. Coleman, J. C., *Unpublished DWPF DCS Data Downloads (SB7b)*, Savannah River Remediation, Aiken, SC, August 2018.

12. Bannochie, C. J., "Tank 40 Final SB7b Chemical Characterization Results," ***SRNL-STI-2012-00097***, ***Rev. 1***, Savannah River National Laboratory, Aiken, SC, November 2012.

13. Johnson, F. C., Crawford, C. L., and Pareizs, J. M., "Analysis of the Sludge Batch 7b (Macrobatch 9) DWPF Pour Stream Glass Sample," ***SRNL-STI-2013-00462, Rev. 0***, Savannah River National Laboratory, Aiken, SC, November 2013.

14. Crawford, C. L., and DiPrete, D. P., "Determination of Reportable Radionuclides for DWPF Sludge Batch 7b (Macrobatch 9)," ***SRNL-STI-2012-00294***, ***Rev. 0***, Savannah River National Laboratory, Aiken, SC, December 2012.

15. Basic Data Report – Defense Waste Processing Facility Sludge Plant, Savannah River Plan 200-S Area, Westinghouse Savannah River Co., Aiken, SC, 1982.

16. Edwards, T. B., *Unpublished MAR Assessment Results*, February 2019.

17. Manara, D., Bhler, R., Boboridis, K., Capriotti, L., Quaini, A., Luzzi, L., Bruycker, F. D., Gueneau, C., Dupin, N., and Konings, R., "The melting behavior of oxide nuclear fuels: effects of the oxygen potential studied by laser heating," ***Procedia Chemistry***, ***7***, 505-512 (2012).

18. Bale, C. W., Bélisle, E., Chartrand, P., Decterov, S. A., Eriksson, G., Gheribi, A. E., Hack, K., Jung, I-H, Kang, Y-B, Melançon, J., Pelton, A.D., Petersen, S., Robelin, C., Sangster, J., Spencer, P., and Van Ende, M-A, "FactSage thermochemical software and databases, 2010-2016," ***CALPHAD: Computer Coupling of Phase Diagrams and Thermochemistry***, **54**, pp 35-53 (2016).

19. Johnson, F. C., Choi, A. S., Miller, D. H., and Immel, D. M., "Comparison of HLW Glass Melting Rate Between Frit and Glass Forming Chemicals Using X-Ray Computed Tomography," ***SRNL-STI-2014-00562, Rev. 0***, Savannah River National Laboratory, Aiken, SC, April 2015.

20. Abramowitz1, H., Calloway, B., Mecholsky N., D'Angelo1, N., Windham, J., and Coleman, J., "Analysis of Bubbled vs. Non-Bubbled DWPF Operating Data," ***SRR-LWP-2018-0002***4, Savannah River Remediation, Aiken, SC, 2013.

21. Vida, J., *The Chemical Behavior of Technetium during the Treatment of High-Level Radioactive Waste,* ***Dissertation, TH Karlsruhe***, 1989 (translation by Hewett, PNL-TR-497).

22. Muller, I. S., Viragh, C., Gan, H., Matlock, K. S., and Pegg, I. L., "Iron Mössbauer redox and relation to technetium retention during vitrification," ***Hyperfine Interactions***, Volume **191**, Issue 1-3, pp 17-24, March 2009.

23. Kim, D., and Kruger, A. A., "Volatile species of technetium and rhenium during waste vitrification," ***J. Non-Crystalline Solids***, **481**, pp 41-50 (2018).

24. Langowski, M. H., Darab, J. G., and Smith, P. A., "Volatility Literature of Chlorine, Iodine, Cesium, Strontium, Technetium, and Rhenium; Technetium and Rhenium Volatility Testing," ***PNNL-11052***, Pacific Northwest National Laboratory, Richland, WA, March 1996.

25. Jantzen, C. M., "Glass Melter Off-Gas System Pluggages: Cause, Significance, and Remediation (U)," ***WSRC-TR-90-205, Rev. 0***, Westinghouse Savannah River Co., Aiken, SC, March 1991.

26. T.H. Lorier and M.E. Smith, "Melt Rate Assessment of SB2/3 with Frit 418 – Effects of Waste Loading and Acid Addition," ***WSRC-TR-2004-00098***, Westinghouse Savannah River Co., Aiken, SC (2004).

27. Choi, A. S., Miller, D. H., Immel, D. M., and Smith, F. G., "Investigation of High-Level Waste Glass Melting Using X-ray Computed Tomography," ***Int. J. Applied Glass Science***, ***8***, Issue 2, pp 165-176 (2016).

28. Data on mass 133 (2265 μg/L) from analysis of MCU Salt Batch 6 vs. Cs-137 by gamma scan (1.28E8 dpm/mL), ***ELN #-A4571-00084-06***, Savannah River National Laboratory, Aiken, SC, November 2015.

29. Mickalonis, J. I., Imrich, K. J., Jantzen, C. M., Murphy, T. R., and Wilderman, J. E., "Corrosion Impact on Alternate Reductant on DWPF and Downstream Facilities," ***SRNL-STI-2014-00281***, ***Rev. 0***, Savannah River National Laboratory, Aiken, SC, December 2014.

30. Choi, A. S., "Melter Off-Gas Flammability Assessment for DWPF Alternate Reductant Flowsheet Options," ***SRNL-STI-2011-00321***, ***Rev. 0***, Savannah River National Laboratory, Aiken, SC, July 2011.

31. Edwards, T. B. (Editor), "SME Acceptability Determination for DWPF Process Control (U)," ***WSRC-TR-95-000364***, ***Rev. 4***, Westinghouse Savannah River Co., Aiken, SC, Augusta 30, 2002.

32. Peeler, D. K., Herman, C. C., Smith, M. E., Lorier, T. H., Best, D. R., Edwards, T. B., and Maich, M. A., "An Assessment of the Sulfate Solubility Limit for the Frit 418 – Sludge Batch 2/3 System," ***WSRC-TR-2004-00081***, ***Rev. 0***, Westinghouse Savannah River Co., Aiken, SC, February 2004.

Distribution:

connie.herman@srnl.doe.gov
joseph.manna@srnl.doe.gov
a.fellinger@srnl.doe.gov
samuel.fink@srnl.doe.gov
gregg.morgan@srnl.doe.gov
boyd.wiedenman@srnl.doe.gov
timothy.brown@srnl.doe.gov
alex.cozzi@srnl.doe.gov
david.crowley@srnl.doe.gov
erich.hansen@srnl.doe.gov
nancy.halverson@srnl.doe.gov
john.mayer@srnl.doe.gov
daniel.mccabe@srnl.doe.gov
frank.pennebaker@srnl.doe.gov
amy.ramsey@srnl.doe.gov
william.ramsey@srnl.doe.gov
michael.stone@srnl.doe.gov
bill.wilmarth@srnl.doe.gov
devon.mcclane@srnl.doe.gov
kevin.fox@srnl.doe.gov
Kathryn.Taylor-Pashow@srnl.doe.gov
david.herman@srnl.doe.gov

joanne_f_grindstaff@orp.doe.gov
christine.langton@srnl.doe.gov
richard.wyrwas@srnl.doe.gov
nicholas.machara@em.doe.gov
kurt.gerdes@em.doe.gov
david_j_swanberg@rl.gov
matthew_r_landon@rl.gov
ridha_b_mabrouki@rl.gov
karthik_subramanian@rl.gov
kaylin_w_burnett@orp.doe.gov
james_j_lynch@orp.doe.gov
elaine_n_diaz@orp.doe.gov
benton_j_ben_harp@orp.doe.gov
stuart_t_arm@rl.gov
mathew.zenkowich@em.doe.gov

Records Administration (EDWS)